Bioorganic & Medicinal Chemistry 24 (2016) 2215–2234

Contents lists available at ScienceDirect

Bioorganic & Medicinal Chemistry

journal homepage: www.elsevier.com/locate/bmc

Purinylpyridinylamino-based DFG-in/αC-helix-out B-Raf inhibitors: Applying mutant versus wild-type B-Raf selectivity indices for compound profiling

Longbin Liu [a,*], Matthew R. Lee [b,†], Joseph L. Kim [c], Douglas A. Whittington [c], Howard Bregman [d], Zihao Hua [d], Richard T. Lewis [d], Matthew W. Martin [d], Nobuko Nishimura [a], Michele Potashman [d], Kevin Yang [a], Shuyan Yi [d], Karina R. Vaida [d], Linda F. Epstein [c], Carol Babij [e], Manory Fernando [e], Josette Carnahan [e], Mark H. Norman [a]

[a] Department of Medicinal Chemistry, Amgen Inc., One Amgen Center Drive, Thousand Oaks, CA 91320, USA
[b] Department of Molecular Structure and Characterization, Amgen Inc., One Amgen Center Drive, Thousand Oaks, CA 91320, USA
[c] Department of Molecular Structure and Characterization, Amgen Inc., 360 Binney St., Cambridge, MA 02142, USA
[d] Department of Medicinal Chemistry, Amgen Inc., 360 Binney St., Cambridge, MA 02142, USA
[e] Department of Oncology Research, Amgen Inc., One Amgen Center Drive, Thousand Oaks, CA 91320, USA

ARTICLE INFO

Article history:
Received 6 February 2016
Revised 20 March 2016
Accepted 27 March 2016
Available online 13 April 2016

Keywords:
B-Raf
Inhibitor
DFG
C-helix
Selectivity
v600e
Wild-type
Sulfonamide

ABSTRACT

One of the challenges for targeting B-Raf^{V600E} with small molecule inhibitors had been achieving adequate selectivity over the wild-type protein B-Raf^{WT}, as inhibition of the latter has been associated with hyperplasia in normal tissues. Recent studies suggest that B-Raf inhibitors inducing the 'DFG-in/αC-helix-out' conformation (Type IIB) likely will exhibit improved selectivity for B-Raf^{V600E}. To explore this hypothesis, we transformed Type IIA inhibitor (**1**) into a series of Type IIB inhibitors (sulfonamides and sulfamides **4**–**6**) and examined the SAR. Three selectivity indices were introduced to facilitate the analyses: the B-Raf^{V600E}/B-Raf^{WT} biochemical (^{b}S), cellular (^{c}S) selectivity, and the phospho-ERK activation (^{P}A). Our data indicates that α-branched sulfonamides and sulfamides show higher selectivities than the linear derivatives. We rationalized this finding based on analysis of structural information from the literature and provided evidence for a monomeric B-Raf-inhibitor complex previously hypothesized to be responsible for the desired B-Raf^{V600E} selectivity.

1. Introduction

The Ras-mitogen activated protein kinase signal pathway Ras ↦ Raf ↦ MEK ↦ ERK regulates cell growth, proliferation, and differentiation. Frequent oncogenic mutations within members of this pathway are closely associated with a number of human cancers. In particular, mutations of the *BRAF* gene occur in approximately 50–70% malignant melanomas, and at lower frequency in thyroid (3%), ovarian (30%), and colon (10%) cancers.[1] Additionally, among the >100 different mutant *BRAF* genes identified, the one with the T1799A mutation, which results in the replacement of valine-600 with glutamic acid in the activation loop in the kinase domain of the B-Raf protein (B-Raf^{V600E}), accounts for 90% of the B-Raf mutations.[2] Relative to wild type B-Raf (B-Raf^{WT}), the B-Raf^{V600E} protein exhibits significantly higher kinase activity (~500×) and elevated ability (~5×) to activate down-stream kinases as measured by the formation of phospho ERK (p-ERK).[3] Thus, B-Raf^{V600E} represents a viable target for the treatment of cancers whose genetic origin stems from activating mutations of the *BRAF* gene, such as malignant melanoma where limited options exist for this extremely aggressive disease.[4]

Since the discovery of the first generation Raf inhibitor sorafenib, much effort has been focused on the design of B-Raf inhibitors with improved intrinsic activity and selectivity over other kinases.[5] Our own work toward this objective resulted in the identification of aminoisoquinoline **1** as a potent and selective B-Raf inhibitor (Fig. 1).[6] The key elements for the enhanced kinase selectivity of **1** reside in: (1) the slightly bulky isoquinoline ring that is better accommodated by the pocket near the X-DFG motif at the beginning

* Corresponding author. Tel.: +1 805 447 3442.
E-mail address: lliu@amgen.com (L. Liu).
† Current address: Lilly Biotechnology Center San Diego, 10300 Campus Point Drive, Suite 200, San Diego, CA 92121, USA.

http://dx.doi.org/10.1016/j.bmc.2016.03.055
0968-0896/

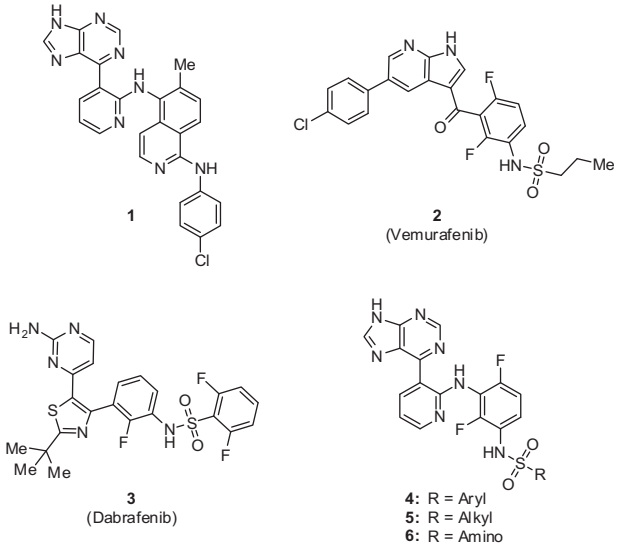

Figure 1. Structures of B-Raf inhibitors (**1**–**3**) and the proposed hybrids (**4**–**6**).

of the activation loop of the B-Raf protein where X is glycine, while in most other kinases a larger amino acid (X) is present; and (2) the 4-Cl substitution in the extended hydrophobic pocket that is less tolerated in some kinases, such as Lck and Tie-2.[6] Compound **1** was equally potent toward both wild-type and mutant B-Raf in the biochemical assays where phosphorylation of MEK1 by the B-Raf proteins were measured (IC_{50} = 2 nM, Table 1).[7] Further investigations revealed that, although compound **1** potently inhibited down-stream ERK phosphorylation (p-ERK, IC_{50} = 2 nM) in A375 cells which harbor the B-Raf^{V600E} protein, it also *activated* the signaling pathway in the human pancreatic carcinoma MIA PaCa-2 cells which carry the B-Raf^{WT} protein (p-ERK, EC_{50} = 22 nM). Extensive in vivo studies revealed that, while administration of **1** resulted in tumor growth inhibition in animal models bearing the human melanoma A375 tumor cells, hyperplasia of normal epithelial cells were also observed.[8] Concurrent to our findings, similar results with other second-generation B-Raf inhibitors appeared in the literature that also suggested that inhibition of B-Raf^{WT} may result in the seemingly paradoxical activation of the MAPK pathway by B-Raf inhibitors.[9] One hypothesis that has been put forth is that, in the presence of high levels of activated Ras protein, the B-Raf^{WT}-inhibitor complex may induce hetero-dimer formation with C-Raf or other RAF family members. The hetero-dimer then *trans*-activates the unoccupied paralogous RAF protomer, resulting in elevated down-stream signaling such as p-ERK.[9c–e,10] The dimerization is required for normal Ras-dependent Raf activation but not for the function of mutants with high catalytic activity, such as Raf^{V600E}. Further, a dimer-interface peptide inhibitor can block both the Raf dimerization and down-stream signaling.[11] Based on this theory, it follows that inhibitors that disfavor dimerization of the B-Raf^{WT}–inhibitor complexes should pose a lower risk of MAPK pathway activation in normal cells, which is associated with hyperplasia in normal tissues, and offer greater therapeutic benefit in the treatment of B-Raf^{V600E} associated cancers. Indeed, a recent study reported the design of PLX-7904/PB04 with increased selectivity for B-Raf^{V600E} over B-Raf^{WT} and impaired hyper-activation of normal MAPK signal.[12]

2. Definition of selectivity indices

Although the direct measure of inhibitor-induced Raf-dimer formation had been described in the mechanistic studies of the paradoxical B-Raf^{WT} pathway activation, it was deemed impractical to be employed in the early stages of SAR exploration.[7] Conceptually, a desirable B-Raf^{V600E} inhibitor would be a compound that exhibits low binding affinity for the B-Raf^{WT} protein (high IC_{50}) relative to its affinity for the target B-Raf^{V600E}. Such a compound must also, besides potently inhibiting the down-stream ERK phosphorylation in the A375 cells that harbor the B-Raf^{V600E} protein, demonstrate minimal or reduced potency (high EC_{50}) in eliciting down-stream ERK phosphorylation in the MIA PaCa-2 cells harboring the B-Raf^{WT} protein. Based on these considerations, two selectivity indices were introduced in our SAR studies: (1) the biochemical selectivity (^{b}S), as measured by the ratio of the IC_{50} values derived from the kinase assays using B-Raf^{WT} and B-Raf^{V600E} enzymes (IC_{50}^{WT}/ IC_{50}^{V600E});[13] (2) the cellular selectivity (^{c}S), as measured by the ratio of the EC_{50} value derived from the MIA PaCa-2 cellular assay and the IC_{50} value derived from the A375 cellular assay (EC_{50}/ IC_{50}). It turns out that in the MIA PaCa-2 cellular assay, the inhibitor-induced maximum p-ERK increase can vary significantly between compounds. Therefore, the percentage of p-ERK activation (^{P}A), defined as the maximum increase of p-ERK relative to baseline control in the MIA PaCa-2 cell assay was also introduced.

Table 1
Comparison of the activity and selectivity of compounds **1**, **2**, and **3**[⊥]

Compd no.	B-Raf^{WT} IC_{50} (nM)	B-Raf^{V600E} IC_{50} (nM)	$^{b}S^{*}$	MIA PaCa-2 EC_{50} (nM)	A375 IC_{50} (nM)	$^{c}S^{\wedge}$	$^{P}A^{\ddagger}$ (%)
1	2	2	1	22	2	11	413
2	20	4	5	2290	17	134	674
3	0.4	1	0.4	529	1	529	755

[⊥] For $n \geqslant 2$, the values are reported as an average and the standard deviations are included in Supporting information.
[*] Biochemical selectivity index (^{b}S) = B-Raf^{WT} IC_{50}/B-Raf^{V600E} IC_{50}.
[^] Cellular selectivity index (^{c}S) = MIA PaCa-2 EC_{50}/A375 IC_{50}.
[‡] p-ERK activation index (^{P}A) = the maximum percentage of p-ERK activation in the MIA PaCa-2 cellular assay relative to control.

While the concept for the biochemical selectivity index (^{b}S) is straightforward, the relationship between the two cellular selectivity indices ^{P}A and ^{c}S can be complicated and is illustrated graphically in Figure 2. By using these selectivity parameters we can compare and contrast different compound profiles to aid in our SAR investigations. For example, if two compounds, X (blue) and Y (red), were similarly potent in the B-Raf^{V600E} cellular assay (i.e., same A375 IC_{50} values) with compound X showing a steeper activation slope and smaller ^{P}A than compound Y in the MIA PaCa-2 assay, the latter would appear to be more specific [$^{c}S(Y) > {}^{c}S(X)$] even though it caused more p-ERK activation [$^{P}A(Y) > {}^{P}A(X)$]. It should be noted that, since the activation curves (hence maximum p-ERK) in the MIA PaCa-2 assay are often not well defined at the top concentrations used in our assay, the corresponding EC_{max} values are not included but are partly reflected in the estimated EC_{50} values.

The value of the selectivity indices is illustrated with the data of compound **1** (Table 1). For example, the biochemical selectivity index ^{b}S for compound **1** is ~1, since it was equally potent inhibiting both the wild-type and the V600E-mutant enzymes; however, the cellular selectivity index (^{c}S) for **1** is 11. Functionally, ^{c}S may be more relevant than ^{b}S, since the former reflects the degree of separation between the inhibition of the B-Raf^{V600E} pathway (hence anti-tumor activity) and the activation of the B-Raf^{WT} pathway (cell growth). Thus, in essence, ^{c}S is a reflection of the 'cellular' safety index of a compound and may be inversely related to a compound's ability to drive Raf protein dimerization. The maximum p-ERK level (^{P}A) for compound **1** was found to be 413% above the baseline control, meaning there was 4-fold pathway activation in B-Raf^{WT} cells. With the selectivity indices for compound **1** established, our goal was then to design compounds with improved selectivity profiles.

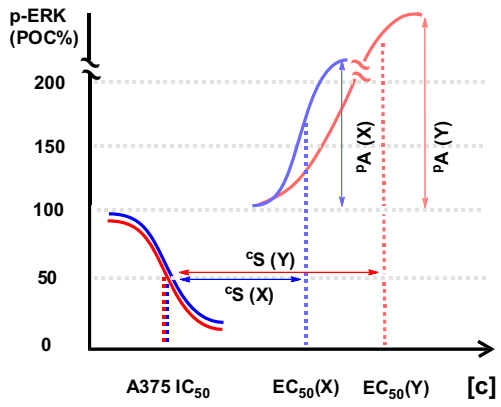

Figure 2. Illustration of how EC_{50} may vary as a function of the slope and the maximum activation in the MIA PaCa-2 assay (^{P}A) for compounds **X** (blue) and **Y** (red) with similar A375 IC_{50}. The cellular selectivity (^{c}S) is determined by the ratio of EC_{50} verses IC_{50} (dark-blue and dark-red curves). Compound **X** appears to be less selective based on its lower EC_{50} value (i.e., smaller ^{c}S) compared to **Y**. On the other hand, **Y** induces a higher percentage of p-ERK (i.e., higher ^{P}A) than **X** in the B-Raf^{WT} cells.

3. Design principle

At the time of our investigation, little was known about how to rationally engineer B-Raf^{V600E} selectivity in an ATP-competitive B-Raf inhibitor since the site of mutation at Val-600 in B-Raf lie outside the ATP binding site. Recently however, sulfonamide-based B-Raf inhibitors have emerged as a class of effective agents in treating patients with malignant melanoma harboring B-Raf^{V600E}, as exemplified by the approval of vemurafenib (**2**)[14] and dabrafenib (**3**).[15] A comparison of the sulfonamides with **1** using the biochemical selectivity index (^{b}S, Table 1) showed that while vemurafenib (**2**) was 5× more selective, dabrafenib (**3**) showed inversed selectivity. Although both **2** and **3** were more selective (>10×) than **1** in the cellular setting (^{c}S), they also showed higher levels of p-ERK induction (^{P}A) in B-Raf^{WT} cells. Thus, considering all three parameters (^{b}S, ^{c}S, and ^{P}A), the selectivity profiles of **2** and **3** are suboptimal and may be responsible for the development of skin lesions in patients after treatment with both therapeutics.[16] We felt that the use of ^{b}S, ^{c}S, and ^{P}A in SAR analysis would facilitate our efforts to improve the selectivity profiles of **1** by identifying compounds that selectively inhibit the B-Raf^{V600E} pathway (i.e., high ^{b}S in biochemical assays and high ^{c}S in cellular assays) and have minimal activation via the B-Raf^{WT} pathway (i.e., low ^{P}A).

Given the superior ^{c}S exhibited by the sulfonamides **2** and **3**, we decided to investigate the sulfonamide pharmacophore within the scaffold defined by **1**. Molecular modeling studies comparing the bound conformations of **1** and **2**[14d] showed that the hinge-binding domains (purine in **1** and pyrrolopyridine in **2**) of both series occupy the same space in the binding pocket of the B-Raf protein (Fig. 3). The mid-section of the molecules link the hinge-binders with the tail groups docking in the extended hydrophobic region, where the binding mode diverges between the two structural classes.[17] The aminoquinoline moiety in **1** forms a hydrogen-bond with Glu501 of the αC-helix and directs the chlorophenyl group towards the extended hydrophobic pocket of the B-Raf^{V600E} protein that, in turn, assumes the inactive DFG-out conformation, despite the *activating* phospo-mimetic nature of Glu600 on the activation loop. In contrast, the sulfonamide moiety in **2** interacts with the backbone amides of both Asp594 and Gly596 and steers the propyl group into the 'Raf-selective' pocket produced by a shift of the αC-helix.[14a] It has been hypothesized that the shift of the αC-helix might be responsible for deterring the formation of B-Raf heterodimers that promote down-stream p-ERK formation. We reasoned that, if the aminoisoquinoline moiety in **1** was replaced with a sulfonamide or sulfamide group, as represented by the generic structures **4**, **5**, and **6**, it may be possible to switch the binding mode from 'DFG-out/αC-helix-in' (Type IIA binder) to 'DFG-in/αC-helix-out' (Type IIB binder) and thereby achieve enhanced B-Raf^{V600E} selectivity. Additionally, we hoped to probe how structural changes in the sulfonamide tail piece would affect each of the selectivity parameters ^{b}S, ^{c}S, and ^{P}A. In this paper, we report the structure–activity relationships and structure–selectivity relationships of the hybrid series. We note that concurrent to our work, other groups had also synthesized compounds identical or similar to some of the examples described here.[18]

4. Synthesis

The sulfonamides **4**–**5** were readily prepared by the methods shown in Scheme 1. In one approach, commercially available 2,6-difluoroaniline (**7**) was protected as the acetamide prior to nitration at the 3-position.[19] The nitro group was reduced under catalytic hydrogenation conditions (H_2, Pd/C) to aniline **8**. The latter was treated with either aryl or alky sulfonyl chlorides in the presence of catalytic amounts of dimethylamino pyridine to furnish the corresponding sulfonamides that were subsequently treated with hydrogen chloride in ethanol to cleave the acetamide group furnishing anilines **9** and **10**, respectively. Alternatively, anilines **9**–**10** were prepared from commercially available 2,4-difluoroaniline (**11**) by first introducing the C-1 sulfonamide functionality followed by installing the C-3 amino group via sequential lithiation–carboxylation, Curtius rearrangement, and Boc-deprotection.[20] The final couplings between anilines **9**–**10** and 6-(2-fluoropyridin-3-yl)-9-(tetrahydro-2*H*-pyran-2-yl)-9*H*-purine **12**[6] were achieved by nucleophilic aromatic substitution (S_NAr) under strongly basic conditions (lithium or sodium hexamethyl disilylazide). The tetrahydropyranyl (THP) protecting group of the purine moiety was cleaved with aqueous hydrogen chloride to give the final products **4a**,**b**,**d**,**g** and **5b**,**d**,**h**,**j**,**k**,**m**,**o**. We also developed a more divergent approach that utilized a common late-stage intermediate for the final sulfonamide analog synthesis. Thus, aniline **11** was first protected as the benzyloxy carbamide (Cbz) prior to the installation of the C-3 amino group as described earlier (e.g., **11** to **9** and **10**), furnishing aniline **13**.[20] S_NAr coupling between **13** and **12**, followed by hydrogenolysis of the Cbz group, afforded the penultimate intermediate aniline **14** that was then functionalized with various aryl or alkyl sulfonyl chlorides to give **4c**,**e**,**f**,**h**–**k** and **5a**,**c**,**e**–**g**,**i**,**l**,**n**,**p** after cleavage of the THP group.

The syntheses of the sulfamide analogs (**6a**–**i**) are shown in Scheme 2. In the first approach, the mono-protected 2,4-difluoro-1,3-diaminobenzene **8** or **15** was treated with sulfuryl chloride and various amines (R^1R^2NH) to install the C-1 sulfamide functionality. Removal of the Boc or Ac protecting group afforded aniline **16**. Alternatively, sulfamide groups were introduced on aniline **11** prior to the introduction of the C-3 amino group using the directed lithiation–carboxylation–Curtis sequence as described earlier for the transformation of **11** to **9** or **10** (Scheme 1). S_NAr coupling between **16** and **12** followed by THP-cleavage afforded analogs **6a**,**b**,**e**,**h**. In the third approach, aniline **14** was directly modified with sulfonyl chloride and amines. This approach was used to prepare analogs **6c**,**d**,**i**. Lastly, aniline **14** was treated with 2-oxooxazolidine-3-sulfonyl chloride,[21] which was generated in situ from the reaction of 2-bromoethanol with chlorosulfonylisocyanate, leading to intermediate **17**. Reaction of the latter with 3-hydroxypyrrolidines gave analogs **6f** and **6g**.

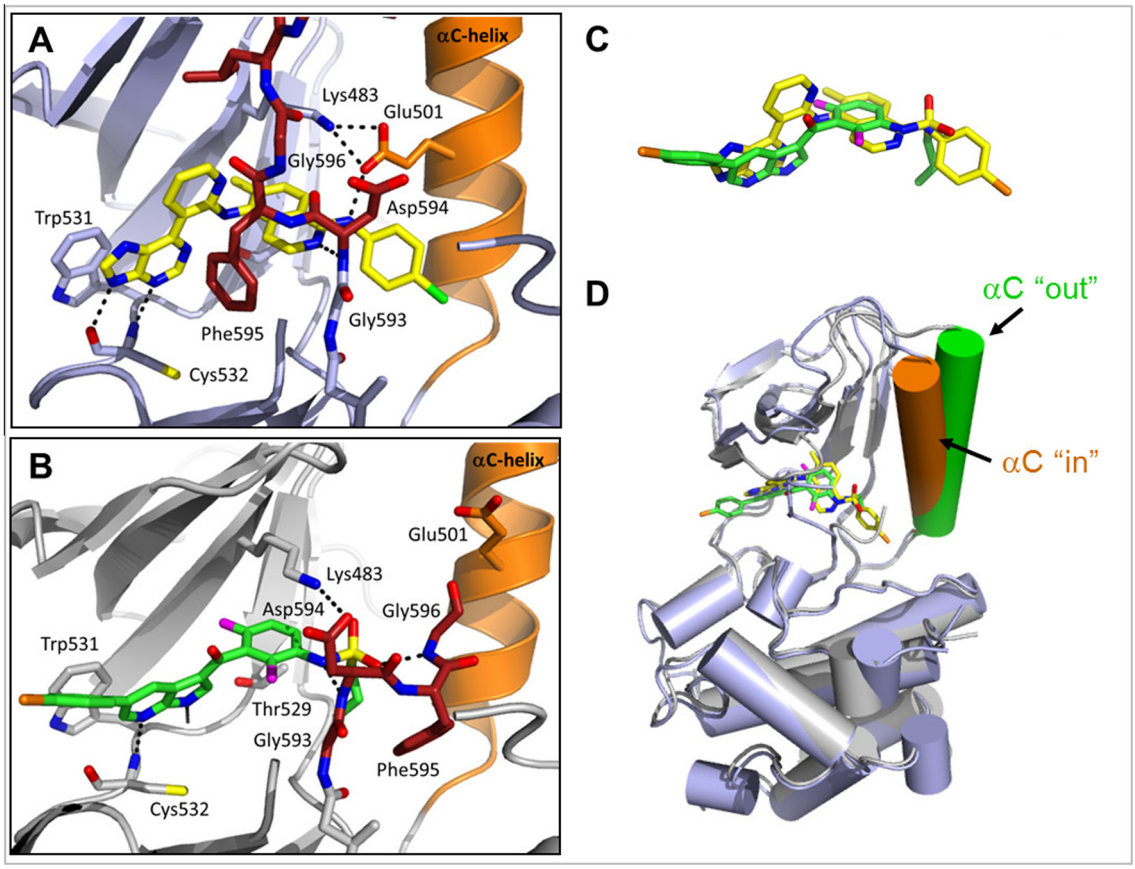

Figure 3. (A) Crystal structure of B-Raf^{V600E} + **1** showing DFG-out, αC-helix-in (Type IIA) binding of the inhibitor (PDB 3IDP). The αC-helix is orange, the activation loop is red, and dashed lines indicate hydrogen bonds. (B) Crystal structure of B-Raf^{V600E} + **2** showing DFG-in, αC-helix-out (Type IIB) binding of the inhibitor, colored as in **A** (PDB 3OG7). (C) Overlay of **1** and **2** based on protein superposition; protein is not depicted for clarity. (D) Overlay of B-Raf^{V600E} + **1** (blue protein, orange αC-helix) and B-Raf^{V600E} + **2** (gray protein, green αC-helix) highlighting the pronounced difference in the αC-helix conformations.

5. Results and discussion

To gauge the impact of replacing an amine with a sulfonamide functionality on B-Raf^{V600E} activity and selectivity, aryl sulfonamides **4a**–**k** were evaluated in comparison with aryl amine **1** (Table 2).[22] In the biochemical assays, phenyl sulfonamide **4a** showed IC_{50} values of 17 and 7 nM toward B-Raf^{WT} and B-Raf^{V600E}, respectively. Compared to **1**, the larger drop of B-Raf^{WT} potency (~8-fold) compared to B-Raf^{V600E} potency (~3.5-fold) resulted in a 2-fold increase in selectivity index ($^{b}S = 2$) in **4a**. In the cellular assays, **4a** was over 100-fold less active than **1** in the wild-type cells (MIA PaCa-2 EC_{50} = 2290 nM) and only 14-fold less potent in the mutant cells (A375 IC_{50} = 28 nM). Therefore, the resulting cellular selectivity ($^{c}S = 82$) was improved by >7-fold over **1**. However, in the MIA PaCa-2 cells, sulfonamide **4a** also induced higher levels of p-ERK activation ($^{p}A = 1540\%$) than **1** ($^{p}A = 413\%$). Thus, the gain of ^{c}S (7-fold) was off-set by the increased ^{p}A (~4-fold) for sulfonamide **4a**. A fluorine substitution at the 2-position of the phenyl ring (**4b**) resulted in slightly higher ^{b}S (3-fold), better cellular potency (but not selectivity), and lower ^{p}A than **4a**. A 3-fluorine substituted analog (**4c**) was as potent and non-selective as **1** in the biochemical assays, although its ^{c}S and ^{p}A were similar to those of **4a**. The 4-fluoro analog (**4d**) showed significant losses in both the biochemical (>18-fold) and the cellular (>100-fold) potencies as well as marginal improvements in ^{b}S and ^{c}S (~2-fold) compared to **1**. Interestingly, the ^{p}A of **4d** was the lowest among the four sulfonamides examined, albeit still higher than that of **1**. With the higher ^{c}S seen from simple phenyl sulfonamides, the effects of heteroaryl sulfonamides were probed. The 3-pyridyl sulfonamide **4e** was more potent than **1** in the biochemical assays but was no more selective. Its cellular potencies and ^{c}S (79) were similar to that of the 2-fluorophenyl analog **4b** but with a higher ^{p}A. Compared to **4e**, the 2-pyridyl analog **4f** was more than 10-fold less potent and showed modest cellular selectivity ($^{c}S = 45$). The 2-thiophene sulfonamide **4g** was more potent than **1** in both the biochemical and the cellular assays. Its cellular selectivity index was modest ($^{c}S = 57$) yet its p-ERK activation in MIA PaCa-2 cells was very high ($^{p}A = 1870$). In comparison, the corresponding thiazole analog **4h** was less potent and selective in the cellular assays ($^{c}S = 25$). Pair-wise analyses of **4h**/**4g** and **4a**/**4f** suggested that aryls containing a nitrogen atom adjacent to the sulfone functionality tended to show eroded cellular potencies and specificities. The 1*H*-pyrazole-4-sulfonamide **4i** exhibited the best potency in both the B-Raf^{V600E} biochemical (IC_{50} = 0.2 nM) and cellular (IC_{50} = 6 nM) assays as well as highest selectivities ($^{b}S = 5$ and $^{c}S = 135$). In contrast, its N-methyl homolog (**4j**) suffered a significant drop in cellular potency (A375 IC_{50} = 710 nM) and selectivity ($^{c}S = 3$). Even more dramatic was the >1000-fold loss in the biochemical potency seen with the 3,5-dimethyl pyrazole analog **4k**. This was likely due to unfavorable conformational penalties imposed by the two methyl groups flanking the sulfonamide group.

The data in Table 2 indicates that, for the aryl sulfonamides (with exceptions for thiazole **4h** and pyrazole **4j**), there is a good

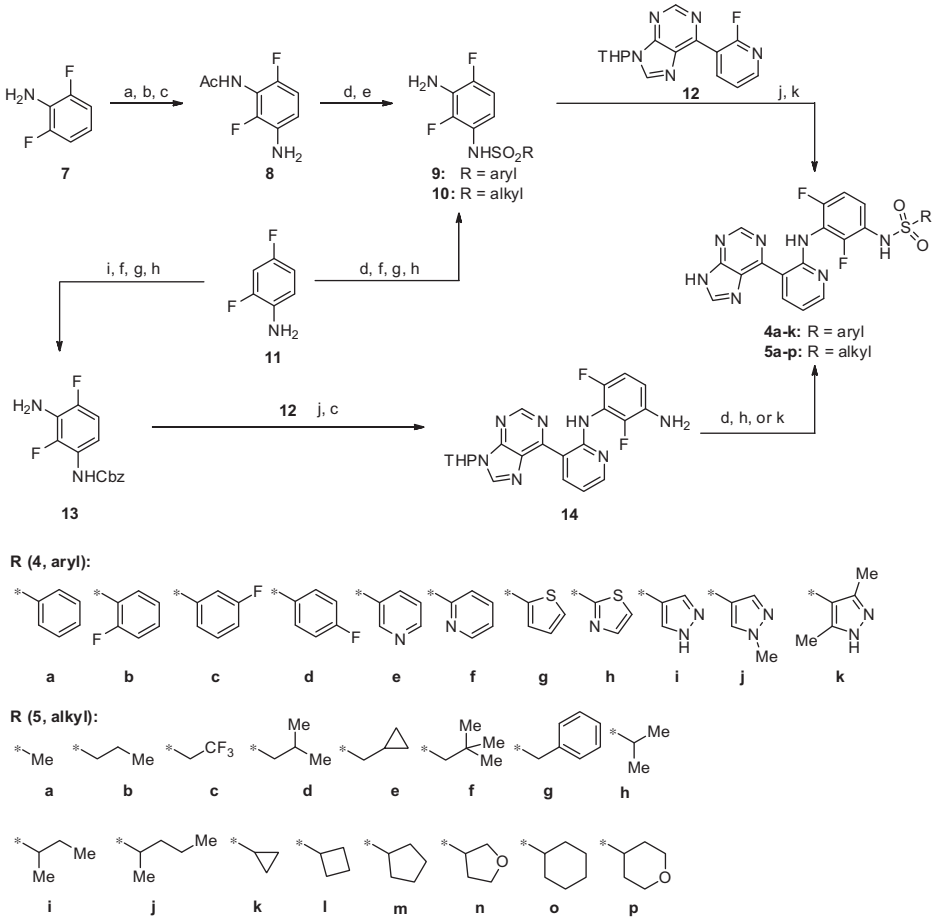

Scheme 1. Synthesis of sulfonamides **4**–**6**. Reagents and conditions: (a) Ac_2O, DCM, rt, 16 h; (b) HNO_3, H_2SO_4, 0 °C → rt, 18 h; (c) H_2, Pd/C (10%), EtOH or EtOAc, rt; (d) RSO_2Cl, Pyr, DMAP, DCM, rt; (e) HCl (aq), EtOH, 90 °C, 16 h; (f) ^{n}BuLi, THF, −78 °C, CO_2; (g) $(PhO)_2P(O)N_3$, Et_3N, ^{t}BuOH, 85 °C; (h) TFA, DCM, rt, or 65 °C; (i) CbzCl, Pyr, DCM, rt, 16 h; (j) NaHMDS or LiHMDS, THF or DMF, 0 °C; (k) HCl (aq), THF, rt.

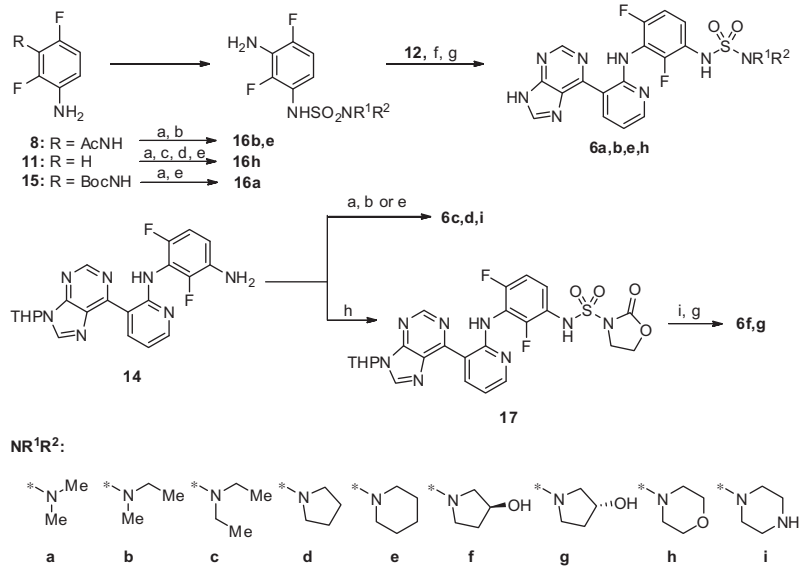

Scheme 2. Synthesis of sulfamides (**6**). Reagents and conditions: (a) R^1R^2NH, SO_2Cl_2, Pyr, DMAP, DCM, −30 °C → rt; (b) HCl (aq), EtOH; (c) ^{n}BuLi, THF, −78 °C, CO_2; (d) $(PhO)_2P(O)N_3$, Et_3N, ^{t}BuOH, 85 °C; (e) TFA, DCM, rt, or 65 °C; (f) NaHMDS or LiHMDS, THF or DMF, 0 °C; (g) HCl (aq), THF, rt; (h) $Cl(SO_2)NCO$, $Br(CH_2)_2OH$, DCM, 0 °C; Et_3N, rt; (i) R^1R^2NH, MeCN, Et_3N, 110 °C.

Table 2
Comparison of the activity and selectivity of aryl sulfonamides **4a–k**[⊥]

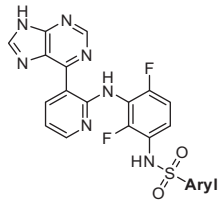

Compd no.	Aryl	B-Raf^{WT} IC_{50} (nM)	B-Raf^{V600E} IC_{50} (nM)	$^{b}S^{*}$	MIA PaCa-2 EC_{50} (nM)	A375 IC_{50} (nM)	$^{c}S^{\wedge}$	$^{p}A^{\ddagger}$ (%)
1	—	2	2	1	22	2	11	413
4a		17	7	2	2290	28	82	1540
4b		10	3	3	873	12	73	989
4c	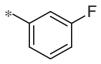	4	3	1	1510	15	101	1470
4d	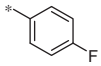	83	36	2	5650	242	23	600
4e		1	1	1	786	10	79	1430
4f		41	21	2	7940	177	45	1110
4g		0.5	1	1	402	7	57	1870
4h		2	1	2	783	31	25	1660
4i		1	0.2	5	807	6	135	1210
4j		19	8	2	2220	710	3	1170
4k		—	216	—	—	—	—	—

A dash (—) sign indicates either non-applicable (e.g. Ar group for **1**) or data unavailable.
[⊥] For $n \geqslant 2$, the values are reported as an average and the standard deviations are included in Supporting information.
[*] Biochemical selectivity index (^{b}S) = B-Raf^{WT} IC_{50}/B-Raf^{V600E} IC_{50}.
[^] Cellular selectivity index (^{c}S) = MIA PaCa-2 EC_{50}/A375 IC_{50}.
[‡] p-ERK activation index (^{p}A) = the maximum percentage of p-ERK activation in the MIA PaCa-2 cellular assay relative to control.

correlation of potencies between the B-Raf^{V600E} biochemical and the A375 cellular assays. In general, the cell-to-enzyme shifts were larger (>5-fold) compared to aryl amine **1**. Most of the aryl sulfonamide analogs exhibited improved cellular selectivities relative to **1**, as judged by the higher ^{c}S values. The increased ^{c}S for the aryl sulfonamides were a direct consequence of the larger separation between the B-Raf^{WT} IC_{50} and the MIA PaCa-2 EC_{50} values than the cellular shifts seen in the B-Raf^{V600E} assays. It is worth noting that there were no correlations between the biochemical (^{b}S) and the cellular (^{c}S) selectivities, as was also shown from the data in Table 1 for the two benchmark compounds (**2** and **3**). Lastly, the maximum level of activation of p-ERK, as indicated by ^{p}A, varied widely (600–1870%) for the aryl sulfonamides and were much higher than for **1**. Since the derived EC_{50} values in the MIA PaCa-2 assay were dependent not only on the slope of the activation curves, but also on the degree of the activation (^{p}A), the value of the cellular selectivity (^{c}S) can be significantly affected by the magnitude of ^{p}A as illustrated in Figure 2. With this in mind, we continued our investigation by examining a series of alkyl sulfonamides and the results are shown in Table 3.

The methyl sulfonamide (**5a**) was only modestly active in the biochemical assays, possibly reflecting the lack of adequate contact in the αC-helix pocket. With a bulkier propyl group as in compound **5b**, low nano-molar IC_{50} values were realized in both the biochemical and the cellular assays. However, **5b** showed no biochemical selectivity (^{b}S = 1), modest cellular selectivity (^{c}S = 39), and high p-ERK activation (^{p}A = 1300). The inferior selectivity of **5b** compared to that of **2** (^{c}S = 134) suggested that structural variation at the hinge-binding region can have significant impact on the B-Raf selectivity. The higher substituted ethyl sulfonamide homologs such as trifluoroethyl (**5c**), isobutyl (**5d**), and cyclopropyl methyl (**5e**) derivatives maintained good A375 cellular potencies (IC_{50} = 17–40 nM) while exhibiting increased ^{b}S and ^{c}S (with the exception of **5c**). These compounds also induced high p-ERK activation in the MIA PaCa-2 cells (1070–1200%). Further increasing the bulkiness to a neo-pentyl group (**5f**) resulted in a loss of selectivity

Table 3
Comparison of the activity and selectivity of alkyl sulfonamides **5a**–**p**[⊥]

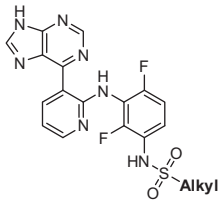

Compd no.	Alkyl	B-Raf^{WT} IC_{50} (nM)	B-Raf^{V600E} IC_{50} (nM)	[b]S[*]	MIA PaCa-2 EC_{50} (nM)	A375 IC_{50} (nM)	[c]S[^]	[P]A[‡] (%)
5a		412	360	1	6690	356	19	1000
5b	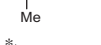	12	9	1	936	24	39	1300
5c		10	3	3	713	40	18	1200
5d	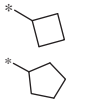	16	6	3	1450	17	85	1100
5e		26	8	3	2140	33	65	1070
5f	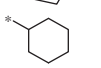	5	6	1	202	63	3	500
5g		111	186	1	5080	>1000	–	517
5h		66	14	5	1540	45	34	356
5i		38	7	5	778	27	29	274
5j	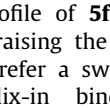	112	18	6	8090	130	62	400
5k		132	41	3	2070	173	12	723
5l		46	4	12	1790	41	44	574
5m	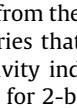	21	2	11	1800	11	164	410
5n		26	5	5	1480	31	48	628
5o		51	18	3	4370	40	109	244
5p		179	31	6	–	356	–	–

A dash (–) sign indicates data unavailable.
[⊥] For $n \geqslant 2$, the values are reported as an average and the standard deviations are included in Supporting information.
[*] Biochemical selectivity index ([b]S) = B-Raf^{WT} IC_{50}/B-Raf^{V600E} IC_{50}.
[^] Cellular selectivity index ([c]S) = MIA PaCa-2 EC_{50}/A375 IC_{50}.
[‡] p-ERK activation index ([P]A) = the maximum percentage of p-ERK activation in the MIA PaCa-2 cellular assay relative to control.

([c]S = 3) and a noticeable reduction of p-ERK activation ([P]A = 500). The overall profile of **5f** resembled aryl amine **1** more than sulfonamides, raising the possibility that the bulky neo-pentyl group might prefer a switch from a DFG-in/ αC-helix-out to a DFG-out/αC-helix-in binding mode. Although the benzyl sulfonamide (**5g**) showed modest biochemical potency, it was inactive in the cellular assays. The isopropyl sulfonamide (**5h**) showed higher [b]S (5-fold) and modest [c]S (34-fold) as compared to the non-α-branched alkyl sulfonamides (**5b**–**5e**). Additionally, this compound also had the lowest level of activation ([P]A 356%) in the MIA PaCa-2 cells. Up to this point, **5h** was the only potent B-Raf inhibitor from the purinylpyridinylamino-2,4-difluorophenyl sulfonamide series that displayed acceptable selectivity based on all three selectivity indices ([b]S, [c]S, and [P]A). This desirable profile seemed to hold for 2-butyl (**5i**) and 2-pentyl (**5j**) derivatives with a slight erosion of the A375 cellular potency from the latter. The cyclopropyl analog (**5k**) showed reduced potency (by 3-fold) and inferior selectivity (2–3-fold in [b]S, [c]S, and [P]A) when compared to the isopropyl derivative (**5h**). However, as the ring size increased as in the 4-, 5-, and 6-membered ring analogs (**5l**,**m**,**o**), both the potency and the selectivity improved. The cyclopentyl analog (**5m**) showed the best combination of [b]S (11-fold) and [c]S (164-fold) while the cyclohexyl analog (**5o**) showed the best combination of [c]S (~110-fold) and [P]A (244%). Cyclic ethers were also examined to explore potential polar interactions as well as to impart improved solubility. It was found that the presence of an oxygen atom led to either reduced cellular selectivity (see, **5n**) or cellular potency (see, **5p**) relative to their corresponding carbocyclic counterparts. The data from Table 3 showed that, like the aryl sulfonamides, there was a good correlation between the biochemical and the cellular IC_{50} values in the B-Raf^{V600E} assays for the alkyl sulfonamides. Similarly, there were no obvious correlations between [b]S and [c]S. However, in contrast to the aryl sulfonamides, lower activation of p-ERK via the wild-type B-Raf pathway was

observed with a majority of the α-branched alkyl sulfonamides (^{P}A < 700%). In this regard, several of these alkyl sulfonamides (**5h**,**i**,**l**,**n**,**o**) performed better than either **2** or **3**.

The favorable ^{P}A profile exhibited by the α-branched alkyl sulfonamides prompted us to examine bis-alkyl sulfamides. We anticipated that the N-substituents of the sulfamides may function as isosteres of the α-branched alkyl groups of the sulfonamides and may also provide structural features inaccessible from either the aryl or the alkyl sulfonamides. As shown in Table 4, *N*,*N*-dimethyl sulfamide **6a** showed cellular potency and selectivity similar to that of isopropyl sulfonamide **5h**. Increasing the sizes of the sulfamide group resulted in reduced cellular potency and selectivity (see, **6b** and **6c**). Cyclic sulfamides seemed to be preferred when compared to the acyclic ones, as suggested by the data for compounds **6c** and **6d**. The five-membered cyclic sulfamide (**6d**) was more potent and selective than the 6-membered sulfamide (**6e**). Heteroatoms were not well tolerated as indicated by the activities of hydroxyprolinyl, morpholinyl, and piperazinyl analogs (**6f**,**g**,**h**,**i**). As was observed with the α-branched alkyl sulfonamides, lower levels of pERK activation in the B-Raf^{WT} pathway (^{P}A ⩽ 600%) were observed with these sulfamides.

Collectively, the data presented for compounds **4**–**6** highlight the challenges of evaluating selectivity profiles of B-Raf^{V600E} inhibitors over the wild-type protein B-Raf^{WT} since the three selectivity indices (^{b}S, ^{c}S, and ^{P}A) each seem to follow their own course of dependency on the structures of the inhibitors. Thus, it became clear that no single selectivity parameter was sufficient for the selection of compounds that would offer maximal B-Raf^{V600E} inhibition while imparting minimal B-Raf^{WT} activation. To help understand the complex structure–selectivity relationships, the biochemical and the cellular selectivity indices (^{b}S and ^{c}S) of the inhibitors from Tables 1–4 were each plotted against the p-ERK activation (^{P}A) in a scatter chart (Fig. 4). The shape of each compound denotes the B-Raf^{V600E} cellular activity (A375 IC_{50}: circle, <55 nM; diamond, >56 nM) and the color codes for its structural type (i.e., compound **1**—orange; aryl sulfonamides—red; α-branched sulfonamides—blue; linear sulfonamides—yellow; sulfamides—green). For the purpose of comparison, the profiles for vemurafenib **2** and dabrafenib **3** were also included in the plots. Additionally, the data points in Figure 4 were divided into four quadrants using aryl amine **1** as the reference point. It is clear that the majority of the analogs showed better biochemical selectivities than **1**. Interestingly, dabrafenib **3** was more potent toward the wild-type than to the mutant B-Raf proteins and was located in the southeast quadrant in Figure 4A whereas vemurafenib **2** occupied the northeastern quadrant due to its high ^{b}S value. Both the aryl and linear alkyl sulfonamides tended to induce high levels of p-ERK (^{P}A) in the wild-type MIA PaCa-2 cells (>600%) and, as a result, occupied the eastern quadrants. By contrast, most of the α-branched analogs showed ^{P}A values <600%. Furthermore, only members from these groups occupy the northwestern quadrant defined by higher ^{b}S and lower ^{P}A with respect to aryl amine **1**. Compounds located within this 'selective quadrant' represent improved selectivity against biochemical affinity and cellular activation and, as shown in Figure 4A, also rank better than **2** and **3** in these regards. With a cellular potency cut-off of 55 nM, compounds

Table 4
Comparison of the activity and selectivity of sulfamides **6a**–**i**[⊥]

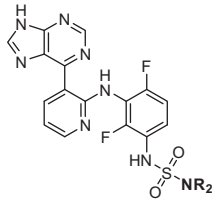

Compd no.	NR_2	B-Raf^{WT} IC_{50} (nM)	B-Raf^{V600E} IC_{50} (nM)	^{b}S[*]	MIA PaCa-2 EC_{50} (nM)	A375 IC_{50} (nM)	^{c}S[^]	^{P}A[‡] (%)
6a		90	8	11	1780	54	33	389
6b		157	22	7	1780	87	20	262
6c		165	57	3	9910	603	16	600
6d		31	2	16	2070	44	47	401
6e		38	15	3	1220	65	19	220
6f	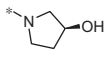	122	9	14	—	201	—	—
6g	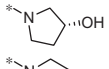	68	16	4	7190	233	31	376
6h		102	62	2	3580	293	12	300
6i		>1000	>1000	—	—	1000	—	—

A dash (—) sign indicates data unavailable.
[⊥] For $n \geqslant 2$, the values are reported as an average and the standard deviations are included in Supporting information.
[*] Biochemical selectivity index (^{b}S) = B-Raf^{WT} IC_{50}/B-Raf^{V600E} IC_{50}.
[^] Cellular selectivity index (^{c}S) = MIA PaCa-2 EC_{50}/A375 IC_{50}.
[‡] p-ERK activation index (^{P}A) = the maximum percentage of p-ERK activation in the MIA PaCa-2 cellular assay relative to control.

5h,**i**,**m**,**o** and **6a**,**d** were readily identified as potent and selective from analogs **4**–**6**. A similar analysis of the cellular selectivity index (^{c}S) as a function of ^{p}A (Fig. 4B) also revealed the same set of potent compounds in the corresponding selective quadrant, albeit in a different rank order along the *y*-axis (^{c}S). In this setting, the two marketed B-Raf inhibitors (**2** and **3**) showed excellent cellular selectivity compared to most of the analogs in Figure 4B. However, in terms of cellular activation (^{p}A), they seem to ranked poor relative to those from the selective quadrant. Thus, we believe that B-Raf inhibitors identified from the selective quadrant may potentially offer larger therapeutic window regarding the off-target safety concerns.

Although we have identified the northwestern quadrant in Figure 4 as the selective quadrant for the type IIB inhibitors described herein, it should be noted that the southwestern quadrant also represents inhibitors with lower activation (^{p}A) of the B-Raf^{WT} pathway albeit also low biochemical (^{b}S) and cellular (^{c}S) selectivity. This set of compounds are interesting in that as the ^{p}A diminishes toward baseline value (0%), both ^{b}S and ^{c}S would become less relevant. As a result, such a compound would still be highly B-Raf^{V600E} specific. Compounds that bind to B-Raf with a slow-off rate and long residence time tend to occupy the southwestern quadrant. An alternative hypothesis to the dimer-transactivation pathway was that fully occupied Raf^{WT}-dimers could not activate the down-stream signaling. Therefore, tighter, pan-Raf binders will induce the formation of dimers whereby both protomers would be completely populated by the inhibitors and thus prevent the undesired activation of the wild type pathway.[23]

6. X-ray crystallography and molecular modeling studies

The intriguing favorable potency and selectivity measures exhibited by the sulfonamides and the sulfamides with branching *alpha* to the sulfone functionality prompted us to investigate their binding to the B-Raf protein. To this end, an X-ray cocrystal structure of B-Raf^{WT} + **6a** was obtained. The crystal structure confirmed the expected mode of binding for the compound based on our initial design considerations, but it also presented an unexpected surprise in that the crystal lattice contained *both* an inhibitor-bound B-Raf^{WT} dimer and an inhibitor-bound B-Raf^{WT} monomer (Fig. 5). In both the monomer and the dimer, the purine ring of **6a** forms two hydrogen bonds to Cys532 in the hinge region of the kinase.

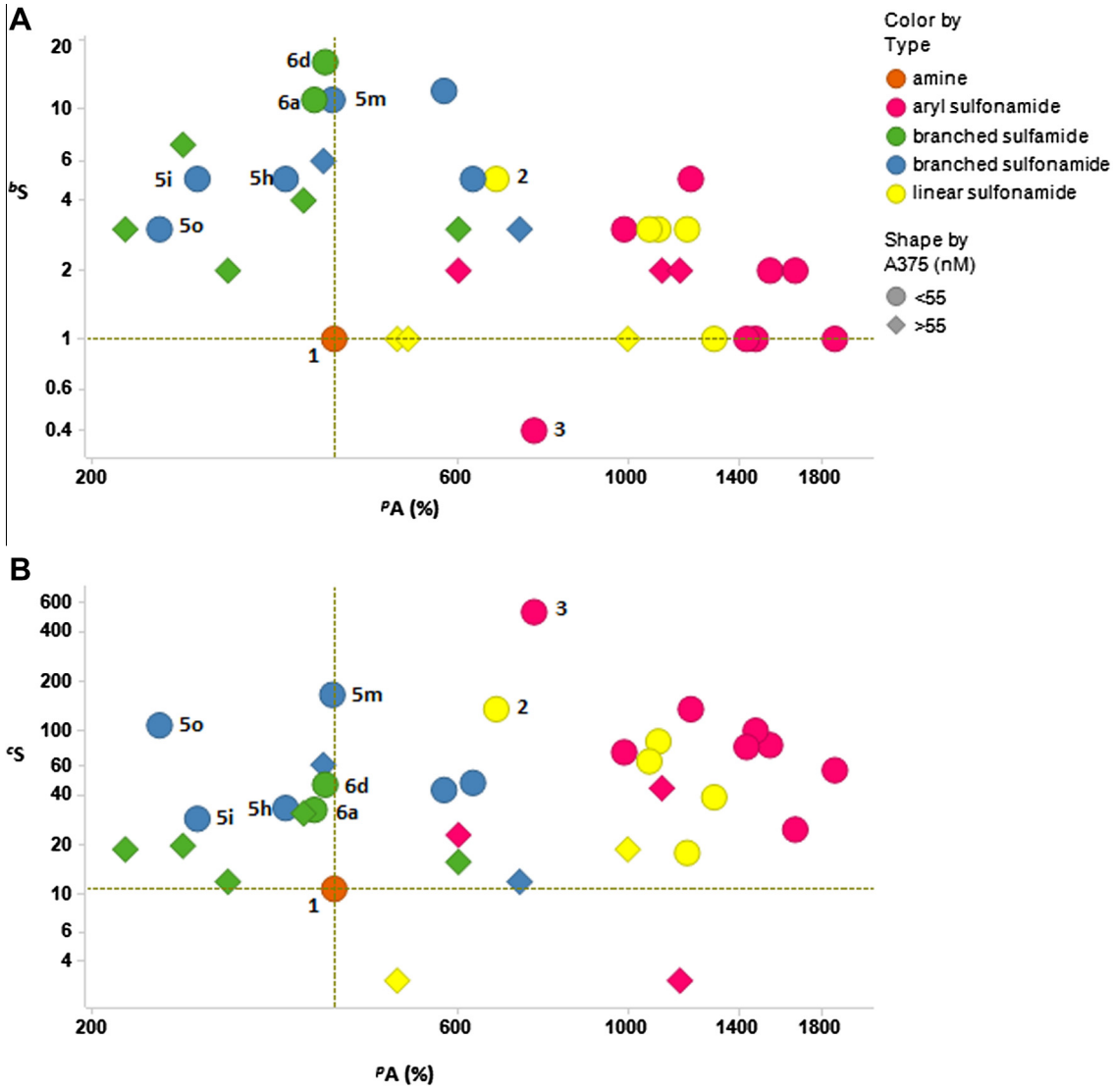

Figure 4. Scatter plot (log scales) of (A): biochemical selectivity (^{b}S) verses p-ERK activation (^{p}A); (B) cellular selectivity (^{c}S) verses p-ERK activation (^{p}A) for analogs from Tables 2–4. The compound-type are color-coded and the A375 cellular potency are represented with either diamonds (0–55 nM) or circles (>56 nM), as shown in the legend in panel (A).

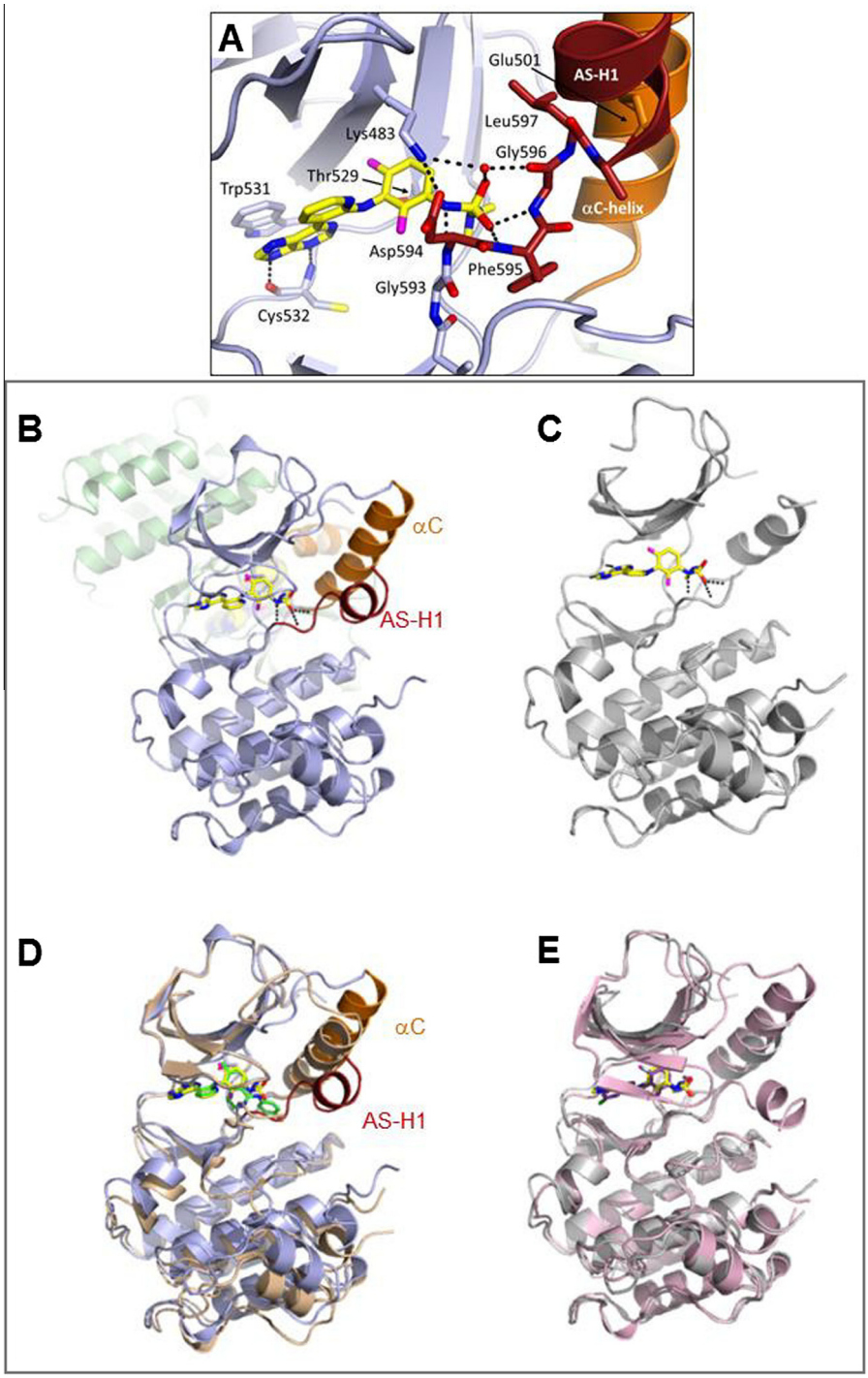

Figure 5. (A) Crystal structure of B-Raf^{WT} + **6a** showing DFG-in/αC-helix-out (Type IIB) binding. The activation loop (red) contains the short AS-H1 helix that helps maintain the αC-helix (orange) in an inactive state. (B) Kinase domain from the crystallographic dimer in the B-Raf^{WT} + **6a** structure colored as in A. The second protein molecule is visible faintly in green. (C) Kinase domain from the crystallographic monomer of B-Raf^{WT} + **6a** showing the greater number of disordered loops (gray dotted lines). (D) Overlay of B-Raf^{WT} + **6a** (colored as in A) with B-Raf^{WT} + **1** (beige; PDB 3IDP). (E) Overlay of the crystallographic monomer of B-Raf^{WT} + **6a** with monomeric structure (PDB: 4WO5, pink).

The difluorophenyl central ring sits in a hydrophobic pocket between gatekeeper residue Thr529 and catalytic Lys483 and occupies approximately the same space as the isoquinoline ring in **1**. The sulfamide nitrogen-atom, in its deprotonated form, serves as a hydrogen bond acceptor for the backbone-NH of Asp594 from the DFG sequence, which assumes the 'in'-conformation.[24] One of the sulfamide oxygen atoms engages in hydrogen bond interactions with the backbone-NHs of both Phe595 and Gly596. The second sulfamide oxygen atom forms a hydrogen bond to an ordered water molecule that in turn interacts with catalytic Lys483 and the backbone carbonyl oxygen atom of Gly596. The dimethyl-nitrogen portion of the sulfamide functionality is oriented 'down' into the Raf-selective pocket at the base of the αC-helix, resulting in the shift of the αC-helix relative to that observed in the DFG-out complex from aryl amine **1** (see the overlay in Fig. 5D). The branched sulfamide is accommodated by a slight enlargement of this pocket resulting from a small shift in the position of the Leu505, Leu514, and Phe595 side chains relative to structures containing inhibitors

bearing a linear propyl sulfonamide group (see Supporting Fig. S1). Overall, the binding mode of **6a** is similar to that of **2.**

The dimer of B-Raf^{WT} + **6a** observed in the crystal lattice is very similar to published structures of other sulfonamide-containing inhibitors in B-Raf,[25] including the presence of an α-helical segment of the activation loop (termed AS-H1) that inserts between the outward shifted αC-helix and the rest of the N-terminal lobe (Fig. 5). As pointed out by others, this protein conformation resembles that of the inactive conformation of the EGFR, ErbB3, and CDK2 kinase domains.[26] A novel aspect of the B-Raf^{WT} + **6a** dimer is that it is formed by a crystallographic two-fold rotation axis (e.g., the two halves of the dimer are identical). In other published structures an entire dimer is contained within one asymmetric unit of the crystal. Whereas the shifted αC-helix in the dimer is well ordered, the corresponding portion of the B-Raf^{WT} + **6a** monomer is much more poorly defined by the electron density. In fact, amino acids from Asn486 to Gln496 in the αC-helix and the preceding loop are missing in the final model and the side chain of Arg509, a residue at the base of the αC-helix that makes important contacts in the B-Raf dimer, is also largely disordered. Additional disorder is observed in the Gly-rich (or P-loop) region of the kinase and in the activation loop beyond the DFG sequence. Overall, despite the disordered regions, the conformation of the monomeric, inhibitor-bound kinase domain aligns quite closely to a recently reported monomer structure of propane-1-sulfonic acid [3-(5-chloro-1*H*-pyrrolo[2,3-*b*]pyridine-3-carbonyl)-2,4-difluorophenyl]amide (PLX4720) + B-Raf^{WT} (Fig. 5E).[26] This similarity includes a slightly larger displacement of the αC-helix relative to its position in the B-Raf dimer structures. Thus, the unique structural features from **6a** complexed to B-Raf^{WT} not only confirmed the association between the αC-helix shift in the B-Raf protein and the high selectivity of the inhibitor for B-Raf^{V600E}, they also provided structural evidence for the existence of monomeric inhibitor–protein complexes that were postulated for the desired inhibition pathway.

However, the αC-helix-out conformation induced by **6a** may not be the only reason for the higher selectivity and lower ERK activation observed from the α-branched sulfonamides and sulfamides since linear sulfonamides also bind to B-Raf protein in this form. An earlier study of a *n*-propyl sulfonamide bound to dimeric B-Raf^{WT} showed that in addition to the DFG-in/αC-helix-out conformation, a second protomer with a DFG-out/αC-helix-in (Type IIA) conformation corresponding to the kinase state permissive to dimerization was also present.[14a] Close examination of this alternative DFG-out binding mode shows that the α-carbon of the propyl group is surrounded by Ile527, Leu505, and Lys483 within 3.5–4.3 Å (Fig. 6). Therefore, an α-substitution at the sulfonamide group would result in unfavorable steric clashes and, as a result, disfavor binding to this DFG-out/αC-helix-in, the 'on' state of the protein. We think that the shifting away from DFG-out/ αC-helix-in toward DFG-in/ αC-helix-out conformation imposed by the α-branched sulfonamides and sulfamides on B-Raf protein is responsible for the better overall selectivity profiles of these inhibitors.[27] In conjunction with our SAR results, these structural analyses suggest that incorporating elements in an inhibitor that favor the αC-helix out-shift and are incompatible with the DFG-in conformation would likely lead to highly selective inhibitors with minimal risk associated with B-Raf^{WT} activation.

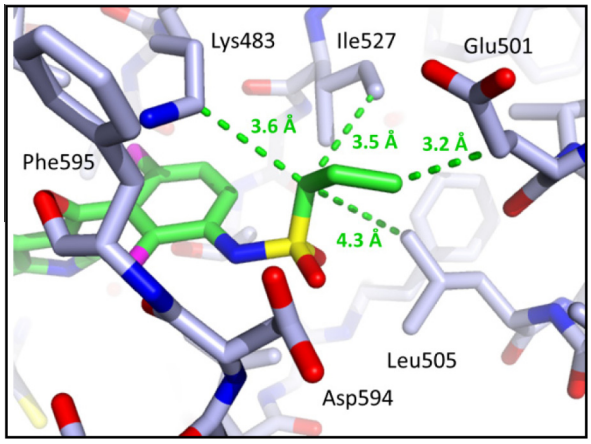

Figure 6. Alternate binding mode of a *n*-propyl sulfonamide inhibitor bound to B-Raf^{WT} (chain B, PDB 3C4C) showing close contacts of the propyl group with the protein.

7. Summary

In the present work, we have shown that, by replacing an aryl amine with various sulfonamides in our previous B-Raf inhibitor, the selectivity profiles towards B-Raf^{V600E} can be significantly altered. Along with the SAR analyses, we discussed the B-Raf^{V600E}/B-Raf^{WT} selectivity based on both the biochemical and the cellular readouts. Our results underscore the complex nature of B-Raf^{V600E} inhibition and B-Raf^{WT} activation, and illustrate the value of using multiple selectivity indices (^{b}S, ^{c}S, and ^{p}A) for compound evaluation and selection. From this study, we were able to identify several α-branched sulfonamide and sulfamide inhibitors (**5h**,**i**,**m**,**o**, **6a**,**d**) that seem to show overall superior selectivity profiles relative to vemurafenib and dabrafenib as well as the original lead (**1**). In addition, these compounds are also selective against other kinases. For example, in the Ambit kinase selectivity scan against a panel of 100 kinases, compound **6a** showed selectivity scores of S(10) = 0.02 and S(35) = 0.03 (see Support information for detail). Thus, the hits identified in this work will serve as useful scaffolds and strategy for future efforts aimed toward optimization of physicochemical properties. A recent report reached similar conclusions concerning the utility of α-branched sulfamide inhibitors as effective inhibitors of paradoxical RAF activation.[28] The co-crystal structure of **6a** in B-Raf^{WT} demonstrated the expected DFG-in/αC-helix-out binding mode, but furthermore, revealed an unexpected mixed B-Raf^{WT} monomer/dimer packing arrangement in the crystals. Both the monomer and the dimer showed inhibitor binding, but the monomeric B-Raf showed extensive disorder in the N-terminal lobe of the kinase that is consistent with a growing body of evidence whereby Raf dimerization and pathway activation are facilitated by an ordered, active kinase conformation.[10b,26] The set of selectivity indices allowed for analysis of mutant/wild-type B-Raf selectivity with respect to both target engagement and target activation. This in turn facilitated the advancement of working hypothesis during the stage of inhibitor design. Finally, X-ray crystallography studies provided structural information for further optimization under the guidance of the selectivity indices. In a broader sense, the concepts presented in this work may be applicable for the design of inhibitors targeting other tumorigenic pathways that deploy compensatory activation mechanisms.

8. Experimental section

8.1. Biological assays

The protocols for the biochemical and cellular assays have been described previously.[7]

8.2. Crystal structure determination

The kinase domain of wild-type B-Raf (433–726) with an N-terminal His_6 affinity tag was expressed in insect cells (Hi-5; Invitrogen) and purified as described previously.[3,6] Purified protein was concentrated to ~3.5 mg/mL using an Ultrafree-0.5 concentrator

(Millipore) in the presence of 0.2 mM compound **6a.** Inhibitor concentration was supplemented to 0.5 mM in the concentrated protein sample prior to cocrystallization experiments. Crystals were grown at room temperature by vapor diffusion in hanging drops consisting of 0.8 μL of protein solution mixed with an equal volume of well solution (16% (w/v) PEG 8000, 10% tacsimate, 0.1 M Tris, pH 8.5). Prior to data collection, crystals were transferred sequentially into mother liquor containing 5–30% ethylene glycol before flash-cooling in liquid nitrogen. X-ray diffraction data were collected at beamline CMCF1-08ID of the Canadian Light Source using a Rayonix 300 CCD detector and $\lambda = 0.9795$ Å. Data were indexed and scaled using HKL2000.[29] The structure was solved by molecular replacement using EPMR[30] and the coordinates of a proprietary B-RAF structure as a search model. Importantly, only monomeric kinase domain search models produced a correct solution. Refinements were performed with REFMAC5[31] as implemented in CCP4[32] and model building was done with COOT.[33] Data collection and refinement statistics appear in Table S3.

8.3. Chemistry

Unless otherwise noted, all reagents and materials were obtained from commercial suppliers and used without further purification. Reactions involving air- or moisture-sensitive reagents were performed under a nitrogen or argon atmosphere. Silica gel chromatography was performed using either glass columns packed with silica gel (200–400 mesh, Aldrich Chemical) or prepacked silica gel cartridges (Biotage or Redisep). NMR spectra were recorded with Bruker spectrometers. Chemical shifts are reported in parts per million (ppm, δ units). All final compounds were purified to $\geqslant$95% purity unless otherwise noted as determined by LCMS (LCAP at 215 nm) obtained on an Agilent 1100 or 1200 spectrometer using one of the following methods: Method A, a gradient of 5–95% acetonitrile in water (containing 0.1% TFA) over 3.5 min on an Agilent SB-C18 column (50 mm × 3.0 mm, 2.5 μm) at 40 °C with a flow rate of 1.5 mL/min; Method B, a gradient of 5–95% acetonitrile in water (containing 0.1% TFA) over 3.5 min on a Waters XBridge C18 column (50 mm × 3.0 mm, 3 μm) at 40 °C with a flow rate of 1.5 mL/min. Low-resolution mass spectrometry (MS) data were obtained using ES ionization mode (positive).

Compounds **2**[14d] and **3**[15] were synthesized according to the literature described methods.

8.3.1. *N*-(3-Amino-2,6-difluorophenyl)acetamide (8)

8.3.1.1. (a) *N*-(2,6-Difluorophenyl)acetamide. To a solution of 2,6-difluoroaniline (16.1 mL, 160 mmol) in DCM (213 mL) was added acetic anhydride (15.8 mL, 170 mmol). The mixture was stirred at rt for 16 h. The reaction mixture was washed with saturated sodium bicarbonate and brine. The organic phase was dried over anhydrous sodium sulfate, and concentrated to give the title compound (26.9 g, 160 mmol, 98%) as a white solid. LCMS (ESI, pos. ion) calcd for $C_8H_7F_2NO$: 171.0; found: 172.2 (M+1).

8.3.1.2. (b) *N*-(2,6-Difluoro-3-nitrophenyl)acetamide. Nitric acid (25.6 mL, 610 mmol) was added to sulfuric acid (53.3 mL, 760 mmol) cooled in an ice-water bath. *N*-(2,6-Difluorophenyl)acetamide (13.0 g, 76.0 mmol) was added. The resulting mixture was stirred at rt for 18 h. The mixture was poured into ice-water and the precipitate was filtered. The solid residue was washed with water and air-dried to give the title compound (11.2 g, 51.8 mmol, 68%) as a yellow solid. LCMS (ESI, pos. ion) calcd for $C_8H_6F_2N_2O_3$: 216.0; found: 217.2 (M+1). ^{1}H NMR (300 MHz, DMSO-d_6) δ ppm 10.04 (br s, 1H), 8.02–8.28 (m, 1H), 7.44 (td, J = 9.1, 1.8 Hz, 1H), 2.11 (s, 3H).

8.3.1.3. (c) *N*-(3-Amino-2,6-difluorophenyl)acetamide (8). In a 150-mL round-bottomed flask under N_2, *N*-(2,6-difluoro-3-nitrophenyl)acetamide (4.10 g, 19.0 mmol) and palladium on carbon (10%, 0.40 g) were mixed with EtOH (119 mL). The reaction mixture was evacuated and refilled with hydrogen (3-times). The mixture was stirred under a balloon pressure of hydrogen at rt for 2 h. The mixture was filtered through a pad of diatomaceous earth and the filtrate was concentrated. The resulting dark residue was absorbed on a plug of silica gel and was purified on silica with NH_3–MeOH (1 M) in DCM (10–100%) to afford the title compound (3.22 g, 17.3 mmol, 91%) as tan solid. LCMS (ESI, pos. ion) calcd for $C_8H_8F_2N_2O$: 186.1; found: 187.1 (M+1). ^{1}H NMR (400 MHz, DMSO-d_6) δ ppm 9.47 (br s, 1H), 6.72–6.87 (m, 1H), 6.56–6.69 (m, 1H), 4.98 (s, 2H), 2.03 (s, 3H).

8.3.2. Method A: General procedure for the synthesis of aryl sulfonamides (9) from 8

To a stirred solution of *N*-(3-amino-2,6-difluorophenyl) acetamide (**8**) in pyridine was added aryl sulfonyl chloride (1.1 equiv) slowly at rt. After being stirred at rt for 1.5 h, the mixture was diluted with water and acidified with aqueous HCl (4 N). The resulting slurry was filtered and the solids were washed with water to afford the crude acetamide intermediate. The intermediate was treated with concentrated hydrogen chloride (15 equiv) in EtOH. The mixture was stirred at 90 °C for 14 h and was concentrated in vacuo. The residue was quenched with saturated sodium bicarbonate and the resulting solid was collected via filtration and washed with water to afford the title product.

8.3.3. *N*-(3-Amino-2,4-difluorophenyl)benzenesulfonamide (9a)

This material was prepared from **8** and benzenesulfonyl chloride according to the procedure described in Method A as brown solid (2.88 g, 94%). Compound **9a** was also prepared from **11** as described in Scheme 1. LCMS (ESI, pos. ion) calcd for $C_{12}H_{10}F_2N_2O_2S$: 284.0; found: 285.0 (M+1). ^{1}H NMR (400 MHz, $CDCl_3$) δ ppm 7.77 (d, J = 7.4 Hz, 2H), 7.60–7.54 (m, 1H), 7.50–7.41 (m, 2H), 6.88 (dt, J = 5.5, 8.7 Hz, 1H), 6.81–6.72 (m, 1H), 6.47 (br s, 1H), 3.66 (br s, 2H).

8.3.4. *N*-(3-(3-(9*H*-Purin-6-yl)pyridin-2-ylamino)-2,4-difluorophenyl)benzenesulfonamide (4a)

8.3.4.1. (a) *N*-(2,4-Difluoro-3-(3-(9-(tetrahydro-2*H*-pyran-2-yl)-9*H*-purin-6-yl)pyridin-2-ylamino)phenyl)benzenesulfonamide. A solution of lithium bis(trimethylsilyl)amide (1.00 M in THF, 1.30 mL, 1.30 mmol) was added dropwise to a solution of *N*-(3-amino-2,4-difluorophenyl)benzenesulfonamide (**9a**, 0.150 g, 0.528 mmol) and 6-(2-fluoropyridin-3-yl)-9-(tetrahydro-2*H*-pyran-2-yl)-9*H*-purine (**12**, 0.174 g, 0.580 mmol) in THF (9.00 mL). After being stirred at rt for 16 h, the reaction mixture was quenched by the addition of HCl (aq, 1 N). The solution was partitioned between ethyl acetate and saturated sodium bicarbonate. The aqueous phase was separated and extracted with ethyl acetate. The combined organic phases were washed with brine, dried over anhydrous sodium sulfate, filtered, and concentrated to afford an orange brown oil. This material was purified via column chromatography on silica gel eluting with ethyl acetate–hexane (0–50%) to afford the title compound (0.178 g, 0.316 mmol, 60%) as tan solid. LCMS (ESI, pos. ion) calcd for $C_{27}H_{23}F_2N_7O_3S$: 563.2; found: 564.2 (M+1).

8.3.4.2. (b) *N*-(3-(3-(9*H*-Purin-6-yl)pyridin-2-ylamino)-2,4-difluorophenyl)benzenesulfonamide (4a). A solution of *N*-(2,4-difluoro-3-(3-(9-(tetrahydro-2*H*-pyran-2-yl)-9*H*-purin-6-yl)pyridin-2-ylamino)phenyl)benzenesulfonamide (0.178 g, 0.316 mmol) in trifluoroacetic acid (3.16 mL) was heated at 65 °C for 2.5 h. The reaction mixture was partitioned between DCM and saturated

sodium bicarbonate. The aqueous phase was extracted with additional DCM. The combined organic phases were washed with brine, dried over anhydrous sodium sulfate, filtered, and concentrated to afford the title compound (**4a**, 0.148 g, 0.309 mmol, 98%) as a tan solid. LCMS (ESI, pos. ion) calcd for $C_{22}H_{15}F_2N_7O_2S$: 479.1; found: 480.2 (M+1). ^{1}H NMR (400 MHz, DMSO-d_6) δ ppm 11.44 (br s, 1H), 9.64 (br s, 1H), 9.00 (s, 1H), 8.71 (s, 1H), 8.15 (dd, J = 4.7, 1.9 Hz, 1H), 7.49–7.84 (m, 6H), 7.05–7.19 (m, 2H), 7.01 (dd, J = 7.8, 4.7 Hz, 1H), 4.38 (br s, 1H).

8.3.4.3. *N*-(3-Amino-2,4-difluorophenyl)-2-fluorobenzenesulfonamide (9b). This material was from **8** and 2-fluorobenzene-1-sulfonyl chloride prepared according to the procedure described in Method A (0.280 g, 61% over two steps). LCMS (ESI, pos. ion) calcd for $C_{12}H_9F_3N_2O_2S$: 302.0; found: 303. (M+1). ^{1}H NMR (400 MHz, DMSO-d_6) δ ppm 10.17 (s, 1H), 7.59–7.79 (m, 2H), 7.39–7.52 (m, 1H), 7.27–7.37 (m, 1H), 6.73–6.86 (m, 1H), 6.33 (dt, J = 5.4, 8.6 Hz, 1H), 5.24 (s, 2H).

8.3.5. *N*-(3-((3-(9*H*-Purin-6-yl)pyridin-2-yl)amino)-2,4-difluorophenyl)-2-fluorobenzenesulfonamide (4b)

This compound was prepared from 6-(2-fluoropyridin-3-yl)-9-(tetrahydro-2*H*-pyran-2-yl)-9*H*-purine (**12**, 0.213 g, 0.713 mmol) and crude *N*-(3-amino-2,4-difluorophenyl)-2-fluorobenzenesulfonamide (**9b**, 0.280 g, 0.926 mmol) using sodium bis(trimethylsilyl) amide (2.85 mL, 2.85 mmol) according to the procedure described for THP-**4a**. The crude intermediate *N*-(2,4-difluoro-3-(3-(9-(tetrahydro-2*H*-pyran-2-yl)-9*H*-purin-6-yl)pyridin-2-ylamino)phenyl)-2-fluorobenzenesulfonamide (0.500 g, 121%) was dissolved in THF (4 mL) and was treated with HCl (aq, 6 N, 0.594 mL, 3.56 mmol) at rt for 16 h. The reaction mixture was diluted with ethyl acetate and quenched with saturated sodium bicarbonate solution. The aqueous phase was extracted with ethyl acetate. The combined organic phases were washed with brine, dried over anhydrous sodium sulfate, filtered, and concentrated. The crude material was purified by chromatography on silica eluting with NH_3–MeOH (1 M) in DCM (1–5%) to provide the title compound (**4b**, 0.082 g, 0.165 mmol, 23%) as yellow solid. LCMS (ESI, pos. ion) calcd for $C_{22}H_{14}F_3N_7O_2S$: 497.1; found: 498.0 (M+1). ^{1}H NMR (400 MHz, DMSO-d_6) δ ppm 13.86 (br s, 1H), 11.48 (br s, 1H), 10.46 (br s, 1H), 9.66 (d, J = 5.2 Hz, 1H), 9.01 (s, 1H), 8.72 (s, 1H), 8.14 (dd, J = 1.8, 4.7 Hz, 1H), 7.67–7.81 (m, 2H), 7.46 (t, J = 9.4 Hz, 1H), 7.36 (t, J = 7.7 Hz, 1H), 7.14 (d, J = 7.8 Hz, 2H), 7.02 (dd, J = 4.7, 7.9 Hz, 1H).

8.3.6. Benzyl 3-amino-2,4-difluorophenylcarbamate (13)

8.3.6.1. (a) Benzyl 2,4-difluorophenylcarbamate. To a 250-mL round-bottomed flask was added 2,4-difluoroaniline (**11**, 4.62 mL, 45.4 mmol), DCM (103 mL) and pyridine (7.40 mL, 91 mmol). The solution was stirred at rt and was treated with benzyl chloroformate (8.15 mL, 54.5 mmol) drop wise via an addition funnel. After being stirred at rt overnight, the mixture was poured into water and was extracted with DCM. The combined extracts were washed with water, brine, dried with anhydrous sodium sulfate, filtered, and concentrated to give the title compound (11.1 g, 42.2 mmol, 93%) as a white solid which was used without further purification. LCMS (ESI, pos. ion) calcd for $C_{14}H_{11}F_2NO_2$: 263.1; found: 286.1 (M+Na). ^{1}H NMR (400 MHz, DMSO-d_6) δ ppm 9.43 (br s, 1H), 7.51–7.66 (m, 1H), 7.24–7.46 (m, 6H), 7.01–7.12 (m, 1H), 5.15 (s, 2H).

8.3.6.2. (b) 3-(Benzyloxycarbonylamino)-2,6-difluorobenzoic acid. To a 250-mL round-bottomed flask under N_2 was added benzyl 2,4-difluorophenylcarbamate (10.7 g, 40.8 mmol) and tetrahydrofuran (100 mL). The solution was cooled at −78 °C and was treated with *n*-butyllithium solution (2.5 M in hexanes, 32.6 mL, 82 mmol) via an addition funnel. The resulting pink solution was stirred at −78 °C for 0.5 h. Dry CO_2 was bubbled through the solution for 1 h. The mixture was stirred at the same temperature for 1 h before the cooling bath was removed. The mixture was poured into ice-water and the organic solvent was evaporated. The aqueous phase was treated with NaOH (1 N) to pH ~10. The basified solution was washed with ethyl acetate. The aqueous layer was treated with HCl (aq, 6 N) to pH ~1. The acidified solution was then extracted with ethyl acetate. The combined extracts were washed with water, brine and dried over anhydrous sodium sulfate. The solvent was evaporated under vacuum and the residue was triturated with hexane to give the title compound (6.99 g, 22.7 mmol, 56%) as a brown solid. LCMS (ESI, pos. ion) calcd for $C_{15}H_{11}F_2NO_4$: 307.1; found: 330.0 (M+Na).

8.3.6.3. (c) Benzyl 3-amino-2,4-difluorophenylcarbamate (13). To a suspension of 3-(benzyloxycarbonylamino)-2,6-difluorobenzoic acid (1.67 g, 5.44 mmol) in *tert*-butanol (27.2 mL, 5.44 mmol) was added triethylamine (1.06 mL, 7.61 mmol). The mixture was stirred for 5 min before diphenyl phosphorazide (1.52 mL, 7.07 mmol) was added. The resulting mixture was stirred at 85 °C overnight. The solvent was evaporated and the residue was dissolved in DCM and cooled to 0 °C. To this cooled solution was added TFA (2.09 mL, 27.2 mmol) and the mixture was stirred at rt for 2.5 h. Additional TFA (3.0 mL) was added and the mixture was stirred at rt overnight. The mixture was diluted with DCM and washed with saturated sodium bicarbonate and brine. The organic phase was dried over anhydrous sodium sulfate, filtered and concentrated. The crude material was absorbed onto a plug of silica gel and purified by chromatography with EtOAc in hexane (0–30%) to afford the title compound (**13**, 0.602 g, 2.17 mmol, 40%) as a yellow solid. LCMS (ESI, pos. ion) calcd for $C_{14}H_{12}F_2N_2O_2$: 278.1; found: 279.2 (M+1). ^{1}H NMR (400 MHz, DMSO-d_6) δ ppm 9.21 (br s, 1H), 7.39–7.47 (m, 4H), 7.28–7.38 (m, 1H), 6.84 (ddd, J = 1.9, 9.0, 10.6 Hz, 1H), 6.60–6.76 (m, 1H), 5.13 (s, 2H).

8.3.7. 2,6-Difluoro-*N*1-(3-(9-(tetrahydro-2*H*-pyran-2-yl)-9*H*-purin-6-yl)pyridin-2-yl)benzene-1,3-diamine (14)

8.3.7.1. (a) Benzyl 2,4-difluoro-3-(3-(9-(tetrahydro-2*H*-pyran-2-yl)-9*H*-purin-6-yl)pyridin-2-ylamino)phenylcarbamate. To a stirred solution of 6-(2-fluoropyridin-3-yl)-9-(tetrahydro-2*H*-pyran-2-yl)-9*H*-purine (**12**, 2.78 g, 9.29 mmol) and benzyl 3-amino-2,4-difluorophenylcarbamate (**13**, 2.84 g, 10.2 mmol) in THF (50 mL) was added sodium bis(trimethylsilyl)amide (1 M in THF, 27.9 mL, 27.9 mmol) at 0 °C dropwise. The dark red mixture was stirred at 0 °C for 30 min. The reaction mixture was partitioned between ethyl acetate and a buffer solution (pH ~5). The aqueous phase was extracted with ethyl acetate. The combined organic phases were washed with brine, dried over anhydrous sodium sulfate, filtered, and concentrated. The crude material was absorbed onto a plug of silica gel and purified by chromatography eluting with EtOAc in hexane (20–60%) to provide the title compound (4.10 g, 7.35 mmol, 79%) as yellow solid.

8.3.7.2. (b) 2,6-Difluoro-*N*1-(3-(9-(tetrahydro-2*H*-pyran-2-yl)-9*H*-purin-6-yl)pyridin-2-yl)benzene-1,3-diamine (14). To a round-bottomed flask with benzyl 2,4-difluoro-3-(3-(9-(tetrahydro-2*H*-pyran-2-yl)-9*H*-purin-6-yl)pyridin-2-ylamino)phenylcarbamate (0.630 g, 1.13 mmol) was added palladium on carbon (10%, 0.120 g), methanol (10 mL) and ethyl acetate (10 mL). The resulting mixture was evacuated-back filled with hydrogen and was stirred at rt under a hydrogen balloon overnight. The solid was filtered and the solution was concentrated. The crude material was absorbed onto a plug of silica gel and purified by chromatography eluting with NH_3–MeOH (1 M) in DCM (0–3%) to provide the title compound (**14**, 0.274 g, 0.647 mmol, 57%) as yellow solid. LCMS (ESI, pos. ion) calcd for $C_{21}H_{19}F_2N_7O$: 423.1; found: 424.2 (M+1). ^{1}H NMR (400 MHz, DMSO-d_6) δ 11.31 (s, 1H), 9.59 (dd, J = 1.9,

7.8 Hz, 1H), 9.07 (s, 1H), 8.94 (s, 1H), 8.20 (dd, *J* = 1.9, 4.7 Hz, 1H), 6.97 (dd, *J* = 4.7, 7.8 Hz, 1H), 6.83 (dt, *J* = 1.7, 9.3 Hz, 1H), 6.61 (dt, *J* = 5.5, 9.3 Hz, 1H), 5.86 (dd, *J* = 2.1, 11.0 Hz, 1H), 4.96 (s, 2H), 3.98–4.11 (m, 1H), 3.67–3.81 (m, 1H), 2.26–2.42 (m, 1H), 1.92–2.10 (m, 2H), 1.70–1.84 (m, 1H), 1.50–1.68 (m, 2H).

8.3.8. Method B: General procedure for the synthesis of sulfonamides (4 and 5) from aniline 14 and sulfonyl chlorides

To a solution of 2,6-difluoro-*N*1-(3-(9-(tetrahydro-2*H*-pyran-2-yl)-9*H*-purin-6-yl)pyridin-2-yl)benzene-1,3-diamine (**14**, 0.150 g, 0.354 mmol) in pyridine (5.0 mL) was added 4-(dimethylamino) pyridine (0.022 g, 0.177 mmol) and aryl or alkyl sulfonyl chloride (0.531 mmol). The resulting mixture was heated at 80 °C under N_2 for 2 h (LCMS was taken to monitor the progress of the reaction). Longer reaction times or more sulfonyl chlorides were necessary in some cases for complete consumption of the aniline. Upon completion of the reaction, the mixture was allowed to cool to rt and was poured into a mixture of EtOAc and ice water. The aqueous layer was extracted with EtOAc and the combined organic phases were dried over anhydrous sodium sulfate and concentrated in vacuo. The crude product was purified by column chromatography to obtain the THP-protected intermediate. Cleavage of the THP was accomplished either with 10% TFA in DCM at rt or with HCl (5 N in THF, 4 equiv) at rt for 2 h. The mixture was neutralized with saturated sodium bicarbonate and was extracted with $CHCl_3$. The organic phase was dried over anhydrous sodium sulfate and concentrated in vacuo. The crude product was purified by column chromatography to afford the final product.

8.3.9. *N*-(3-((3-(9*H*-Purin-6-yl)pyridin-2-yl)amino)-2,4-difluorophenyl)-3-fluorobenzenesulfonamide (4c)

This compound was prepared in a one-pot variation from **14** and 3-fluorobenzene-1-sulfonyl chloride according to the procedure described in Method B as a white powder (13.0 mg, 0.0262 mmol, 19%). LCMS (ESI, pos. ion) calcd for $C_{22}H_{14}F_3N_7O_2S$: 497.1; found: 498.0 (M+1). ^{1}H NMR (500 MHz, DMSO-d_6) δ ppm 11.46 (d, *J* = 11.9 Hz, 1H), 9.65 (br s, 1H), 8.99 (s, 1H), 8.70 (s, 1H), 8.14 (dd, *J* = 1.9, 4.6 Hz, 1H), 7.61–7.69 (m, 1H), 7.59 (d, *J* = 7.8 Hz, 1H), 7.50–7.56 (m, 2H), 7.09–7.17 (m, 2H), 7.01 (dd, *J* = 4.8, 7.8 Hz, 1H).

8.3.10. *N*-(3-Amino-2,4-difluorophenyl)-4-fluorobenzenesulfonamide (9d)

This material was prepared from **8** and 4-fluorobenzene-1-sulfonyl chloride prepared according to the procedure described in Method A as yellow solid (0.38 g, 88% over two steps). LCMS (ESI, pos. ion) calcd for $C_{12}H_9F_3N_2O_2S_2$: 302.0; found: 303.0 (M+1). ^{1}H NMR (400 MHz, DMSO-d_6) δ ppm 9.86 (s, 1H), 9.81–9.91 (m, 1H), 7.60–7.74 (m, 2H), 7.60–7.74 (m, 2H), 7.60–7.74 (m, 2H), 7.30–7.40 (m, 2H), 6.74 (ddd, *J* = 10.6, 8.9, 1.9 Hz, 1H), 6.24 (td, *J* = 8.6, 5.5 Hz, 1H), 5.17 (s, 2H).

8.3.11. *N*-(3-((3-(9*H*-Purin-6-yl)pyridin-2-yl)amino)-2,4-difluorophenyl)-4-fluorobenzenesulfonamide (4d)[18d]

This compound was prepared from **9d** and **12** according to the sequence described for **4b** (61.0 mg, 0.123 mmol, 13%). LCMS (ESI, pos. ion) calcd for $C_{22}H_{14}F_3N_7O_2S$: 497.1; found: 498.0 (M+1). ^{1}H NMR (400 MHz, DMSO-d_6) δ ppm 11.44 (d, *J* = 6.2 Hz, 1H), 9.63 (br s, 1H), 9.00 (s, 1H), 8.71 (s, 1H), 8.15 (dd, *J* = 1.9, 4.8 Hz, 1H), 7.74–7.89 (m, 2H), 7.42 (t, *J* = 8.8 Hz, 2H), 7.07–7.14 (m, 2H), 7.02 (dd, *J* = 4.7, 7.8 Hz, 1H).

8.3.12. *N*-(3-((3-(9*H*-Purin-6-yl)pyridin-2-yl)amino)-2,4-difluorophenyl)pyridine-3-sulfonamide (4e)[18a]

This compound was prepared from **14** and pyridine-3-sulfonyl chloride according to the procedure described in Method B as a yellow solid (TFA salt, 37.0 mg, 0.0620 mmol, 22%). LCMS (ESI, pos. ion) calcd for $C_{21}H_{14}F_2N_8O_2S$: 480.1; found: 481.0 (M+1). ^{1}H NMR (400 MHz, DMSO-d_6) δ ppm 11.45 (br s, 1H), 9.64 (br s, 1H), 9.00 (s, 1H), 8.87 (d, *J* = 1.8 Hz, 1H), 8.81 (dd, *J* = 1.4, 4.7 Hz, 1H), 8.72 (s, 1H), 8.15 (dd, *J* = 1.9, 4.7 Hz, 1H), 8.11 (td, *J* = 2.0, 8.1 Hz, 1H), 7.62 (dd, *J* = 4.6, 7.7 Hz, 1H), 7.07–7.20 (m, 2H), 7.02 (dd, *J* = 4.7, 7.9 Hz, 1H).

8.3.13. *N*-(3-((3-(9*H*-Purin-6-yl)pyridin-2-yl)amino)-2,4-difluorophenyl)pyridine-2-sulfonamide (4f)

This compound was prepared from **14** and pyridine-2-sulfonyl chloride according to the procedure described in Method B as a light-yellow powder (25.0 mg, 0.0520 mmol, 22%). LCMS (ESI, pos. ion) calcd for $C_{21}H_{14}F_2N_8O_2S$: 480.1; found: 481.0 (M+1). ^{1}H NMR (400 MHz, DMSO-d_6) δ ppm 12.08 (s, 1H), 9.79 (dd, *J* = 1.8, 7.7 Hz, 1H), 8.59 (s, 1H), 8.52 (d, *J* = 4.50 Hz, 1H), 8.07 (s, 1H), 8.01 (dd, *J* = 1.8, 4.6 Hz, 1H), 7.79–7.90 (m, 2H), 7.30–7.41 (m, 1H), 7.09 (dt, *J* = 6.1, 9.1 Hz, 1H), 6.82 (dd, *J* = 4.7, 7.6 Hz, 1H), 6.61 (t, *J* = 8.8 Hz, 1H).

8.3.14. *N*-(3-Amino-2,4-difluorophenyl)thiophene-2-sulfonamide (9g)

This material was prepared from **8** and thiophene-2-sulfonyl chloride according to the procedure described in Method A as yellow solid (0.330 g, 1.14 mmol, 97%). LCMS (ESI, pos. ion) calcd for $C_{10}H_8F_2N_2O_2S_2$: 290.0; found: 291.0 (M+1). ^{1}H NMR (400 MHz, DMSO-d_6) δ ppm 10.03 (s, 1H), 7.93 (dd, *J* = 1.4, 5.0 Hz, 1H), 7.47 (dd, *J* = 1.4, 3.7 Hz, 1H), 7.15 (dd, *J* = 3.7, 5.0 Hz, 1H), 6.83 (ddd, *J* = 2.0, 8.90, 10.7 Hz, 1H), 6.35 (dt, *J* = 5.5, 8.6 Hz, 1H), 5.24 (s, 2H).

8.3.15. *N*-(3-((3-(9*H*-Purin-6-yl)pyridin-2-yl)amino)-2,4-difluorophenyl)thiophene-2-sulfonamide (4g)[18a]

This compound was prepared from **9g** and **12** according to the sequence described for **4b** as an amorphous solid (0.180 g, 0.371 mmol, 43%). LCMS (ESI, pos. ion) calcd for $C_{20}H_{13}F_2N_7O_2S_2$: 485.1; found: 486.0 (M+1). ^{1}H NMR (400 MHz, DMSO-d_6) δ ppm 13.90 (br s, 1H), 11.57 (s, 1H), 10.39 (br s, 1H), 9.74 (d, *J* = 7.9 Hz, 1H), 9.09 (s, 1H), 8.79 (s, 1H), 8.25 (dd, *J* = 1.9, 4.7 Hz, 1H), 8.03 (dd, *J* = 1.4, 5.0 Hz, 1H), 7.59 (dd, *J* = 1.4, 3.7 Hz, 1H), 7.16–7.29 (m, 3H), 7.09 (dd, *J* = 4.7, 7.9 Hz, 1H).

8.3.16. *N*-(2,4-Difluoro-3-(3-(9-(tetrahydro-2*H*-pyran-2-yl)-9*H*-purin-6-yl)pyridin-2-ylamino)phenyl)thiazole-2-sulfonamide (4h)

This compound was prepared from **14** and thiazole-2-sulfonyl chloride according to the procedure described in Method B as an amorphous solid (0.062 g, 0.13 mmol, 69%). LCMS (ESI, pos. ion) calcd for $C_{19}H_{12}F_2N_8O_2S_2$: 486.1; found: 486.8. (M+1). ^{1}H NMR (300 MHz, DMSO-d_6) δ ppm 13.85 (br s, 1H), 11.52 (s, 1H), 10.89 (s, 1H), 9.67 (dd, *J* = 7.8, 1.5 Hz, 1H), 9.02 (s, 1H), 8.72 (s, 1H), 8.14–8.24 (m, 2H), 8.11 (d, *J* = 3.1 Hz, 1H), 7.11–7.26 (m, 2H), 7.02 (dd, *J* = 7.9, 4.7 Hz, 1H).

8.3.17. *N*-(3-(3-(9*H*-Purin-6-yl)pyridin-2-ylamino)-2,4-difluorophenyl)-1*H*-pyrazole-4-sulfonamide hydrochloride (4i)

This compound was prepared from **14** and *1H*-pyrazole-4-sulfonyl chloride according to the procedure described in Method B as an amorphous solid (40 mg, 0.079 mmol, 22%). LCMS (ESI, pos. ion) calcd for $C_{19}H_{13}F_2N_9O_2S$: 469.1; found: 470.0. (M+1). ^{1}H NMR (400 MHz, DMSO-d_6) δ ppm 11.50 (br s, 1H), 9.92 (s, 1H), 9.64 (d, *J* = 7.2 Hz, 1H), 9.03 (s, 1H), 8.73 (s, 1H), 8.20 (dd, *J* = 1.9, 4.7 Hz, 1H), 7.98 (br s, 2H), 7.10–7.26 (m, 2H), 7.04 (dd, *J* = 4.7, 7.7 Hz, 1H).

8.3.18. *N*-(3-(3-(9*H*-Purin-6-yl)pyridin-2-ylamino)-2,4-difluorophenyl)-1-methyl-1*H*-pyrazole-4-sulfonamide(4j)[18a]

This compound was prepared from **14** and 1-methyl-*1H*-pyrazole-4-sulfonyl chloride according to the procedure described in

Method B as an amorphous solid (60.0 mg, 0.124 mmol, 35%). LCMS (ESI, pos. ion) calcd for $C_{20}H_{15}F_2N_9O_2S$: 483.1; found: 484.1 (M+1). ^{1}H NMR (400 MHz, DMSO-d_6) δ ppm 11.54 (br s, 1H), 9.84–10.17 (m, 1H), 9.74 (br s, 1H), 9.07 (s, 1H), 8.77 (s, 1H), 8.25 (td, J = 1.8, 3.1 Hz, 2H), 7.74 (d, J = 0.8 Hz, 1H), 7.15–7.30 (m, 2H), 7.09 (dd, J = 4.7, 7.8 Hz, 1H), 3.91 (s, 3H).

8.3.19. *N*-(3-(3-(9*H*-Purin-6-yl)pyridin-2-ylamino)-2,4-difluorophenyl)-3,5-dimethyl-1*H*-pyrazole-4-sulfonamide (4k)

This compound was prepared from **14** and 3,5-dimethyl-*1H*-pyrazole-4-sulfonyl chloride according to the procedure described in Method B (30 mg, 0.060 mmol, 20%) as a light-yellow powder. LCMS (ESI, pos. ion) calcd for $C_{21}H_{17}F_2N_9O_2S$: 497.1; found: 498.0 (M+1). ^{1}H NMR (400 MHz, DMSO-d_6) δ ppm 13.65–14.06 (bs, 1H), 12.86 (s, 1H), 11.46 (br s, 1H), 9.50–9.95 (m, 2H), 9.02 (s, 1H), 8.72 (s, 1H), 8.19 (dd, J = 1.9, 4.7 Hz, 1H), 7.07–7.25 (m, 2H), 7.02 (dd, J = 4.7, 7.9 Hz, 1H), 2.15 (br s, 6H).

8.3.20. *N*-(3-(3-(9*H*-Purin-6-yl)pyridin-2-ylamino)-2,4 difluorophenyl)methanesulfonamide (5a)[15,18a]

This compound was prepared from **14** and methanesulfonyl chloride according to the procedure described in Method B as an amorphous solid (17 mg, 0.041 mmol, 68%). LCMS (ESI, pos. ion) calcd for $C_{17}H_{13}F_2N_7O_2S$: 417.1; found: 417.8 (M+1). ^{1}H NMR (300 MHz, MeOH-d_4) δ ppm 9.53 (br s, 1H), 9.00 (s, 1H), 8.52 (s, 1H), 8.15 (dd, J = 4.8, 1.8 Hz, 1H), 7.32–7.42 (m, 1H), 7.07 (td, J = 9.2, 2.0 Hz, 1H), 6.98–7.03 (m, 1H), 3.03 (s, 3H).

8.3.21. *N*-(3-Amino-2,4-difluorophenyl)propane-2-sulfonamide (10b)

This material was prepared from **8** and propane-2-sulfonyl according to the procedure described in Method A as white solid (0.430 g, 1.72 mmol, 57% overall). LCMS (ESI, pos. ion) calcd for $C_9H_{12}F_2N_2O_2S$: 250.1; found: 251.2 (M+1). ^{1}H NMR (400 MHz, DMSO-d_6) δ ppm 9.35 (s, 1H), 6.87 (ddd, J = 2.0, 8.9, 10.7 Hz, 1H), 6.52 (dt, J = 5.5, 8.7 Hz, 1H), 5.31 (s, 2H), 2.96–3.07 (m, 2H), 1.66–1.83 (m, 2H), 0.98 (t, J = 7.4 Hz, 3H).

8.3.22. *N*-(3-(3-(9*H*-Purin-6-yl)pyridin-2-ylamino)-2,4-difluorophenyl)propane-1-sulfonamide (5b)[18a,18d]

This compound was prepared from **10b** and **12** according to the sequence described for **4b** as an amorphous solid (0.203 g, 0.456 mmol, 62%). LCMS (ESI, pos. ion) calcd for $C_{19}H_{17}F_2N_7O_2S$: 445.1; found: 446.0 (M+1). ^{1}H NMR (400 MHz, DMSO-d_6) δ ppm 13.87 (br s, 1H), 11.58 (s, 1H), 9.61–9.75 (m, 2H), 9.04 (s, 1H), 8.74 (s, 1H), 8.20 (dd, J = 1.8, 4.7 Hz, 1H), 7.29 (dt, J = 5.7, 8.7 Hz, 1H), 7.12–7.23 (m, 1H), 7.04 (dd, J = 4.7, 7.9 Hz, 1H), 3.01–3.13 (m, 2H), 1.67–1.83 (m, 2H), 0.98 (t, J = 7.4 Hz, 3H).

8.3.23. *N*-(3-(3-(9*H*-Purin-6-yl)pyridin-2-ylamino)-2,4-difluorophenyl)-2,2,2-trifluoroethanesulfonamide (5c)[18d]

This compound was prepared from **14** and 2,2,2-trifluoroethanesulfonyl chloride according to the procedure described in Method B as an amorphous solid (65 mg, 0.13 mmol, 54%). LCMS (ESI, pos. ion) calcd for $C_{18}H_{12}F_5N_7O_2S$: 485.1; found: 486.0 (M+1). ^{1}H NMR (300 MHz, DMSO-d_6) δ ppm 11.58 (br s, 1H), 10.33 (br s, 1H), 9.70 (d, J = 7.4 Hz, 1H), 9.03 (s, 1H), 8.73 (s, 1H), 8.20 (dd, J = 4.7, 1.9 Hz, 1H), 7.33 (td, J = 8.7, 5.7 Hz, 1H), 7.14–7.27 (m, 1H), 7.04 (dd, J = 7.8, 4.8 Hz, 1H), 4.52 (q, J = 9.8 Hz, 2H).

8.3.24. *N*-(3-Amino-2,4-difluorophenyl)-2-methylpropane-1-sulfonamide (10d)

This material was prepared from **8** and isopropylsulfonyl chloride according to the procedure described in Method A as colorless oil (0.430 g, 1.63 mmol, 61%). LCMS (ESI, pos. ion) calcd for $C_{10}H_{14}F_2N_2O_2S$: 264.1; found: 265.1 (M+1). ^{1}H NMR (300 MHz, $CDCl_3$) δ ppm 6.73–6.98 (m, 2H), 6.28 (br s, 1H), 3.83 (br s, 2H), 2.98 (d, J = 6.6 Hz, 2H), 2.31 (dt, J = 13.4, 6.7 Hz, 1H), 1.10 (d, J = 6.7 Hz, 6H).

8.3.25. *N*-(3-(3-(9*H*-Purin-6-yl)pyridin-2-ylamino)-2,4-difluorophenyl)-2-methylpropane-1-sulfonamide (5d)[18a]

This compound was prepared from **9** and **10h** according to the sequence described for **4b** as an amorphous solid (0.110 g, 0.239 mmol, 87%). LCMS (ESI, pos. ion) calcd for $C_{20}H_{19}F_2N_7O_2S$: 459.1; found: 460.1 (M+1). ^{1}H NMR (300 MHz, DMSO-d_6) δ ppm 11.57 (s, 1H), 9.70 (dd, J = 7.8, 1.7 Hz, 1H), 9.64 (s, 1H), 9.03 (s, 1H), 8.73 (s, 1H), 8.20 (dd, J = 4.7, 1.8 Hz, 1H), 7.29 (td, J = 8.7, 5.8 Hz, 1H), 7.13–7.22 (m, 1H), 7.04 (dd, J = 7.8, 4.8 Hz, 1H), 3.01 (d, J = 6.4 Hz, 2H), 2.19 (dt, J = 13.3, 6.6 Hz, 1H), 1.03 (d, J = 6.7 Hz, 6H).

8.3.26. *N*-(3-(3-(9*H*-Purin-6-yl)pyridin-2-ylamino)-2,4-difluorophenyl)-1-cyclopropylmethanesulfonamide (5e)

This compound was prepared from **14** and cyclopropylmethanesulfonyl chloride according to the procedure described in Method B as an amorphous solid (27.8 mg, 0.060 mmol, 20%). LCMS (ESI, pos. ion) calcd for $C_{20}H_{17}F_2N_7O_2S$: 457.1; found: 458.0 (M+1). ^{1}H NMR (500 MHz, DMSO-d_6) δ ppm 9.52 (s, 1H), 9.04 (s, 1H), 8.72 (s, 1H), 8.20 (dd, J = 4.6, 1.9 Hz, 1H), 7.26 (td, J = 8.8, 5.4 Hz, 1H), 7.10–7.19 (m, 1H), 7.02–7.09 (m, 1H), 3.86–3.95 (m, 1H), 3.50 (s, 2H), 3.17 (s, 1H), 2.21–2.36 (m, 4H), 1.85–1.98 (m, 2H).

8.3.27. *N*-(3-(3-(9*H*-Purin-6-yl)pyridin-2-ylamino)-2,4-difluorophenyl)-2,2-dimethylpropane-1-sulfonamide (5f)

This compound was prepared from **14** and 2,2-dimethylpropane-1-sulfonyl chloride according to the procedure described in Method B as an amorphous solid (2.9 mg, 0.006 mmol, 2%). LCMS (ESI, pos. ion) calcd for $C_{21}H_{21}F_2N_7O_2S$: 473.1; found: 474.2 (M+1). ^{1}H NMR (500 MHz, DMSO-d_6) δ ppm 11.51 (br s, 1H), 9.64 (br s, 1H), 9.03 (s, 1H), 8.71 (s, 1H), 8.19 (dd, J = 4.8, 1.9 Hz, 1H), 7.25–7.35 (m, 1H), 7.13–7.22 (m, 1H), 7.03 (dd, J = 7.8, 4.6 Hz, 1H), 3.08 (s, 2H), 1.10 (s, 9H).

8.3.28. *N*-(3-(3-(9*H*-Purin-6-yl)pyridin-2-ylamino)-2,4-difluorophenyl)-1-phenylmethanesulfonamide (5g)

This compound was prepared from **14** and phenylmethanesulfonyl chloride according to the procedure described in Method B as an amorphous solid (130 mg, 0.263 mmol, 44%). LCMS (ESI, pos. ion) calcd for $C_{23}H_{17}F_2N_7O_2S$: 493.1; found: 494.0 (M+1). ^{1}H NMR (400 MHz, DMSO-d_6) δ ppm 11.56 (br s, 1H), 9.70 (br s, 2H), 9.05 (s, 1H), 8.73 (s, 1H), 8.21 (dd, J = 4.7, 1.8 Hz, 1H), 7.31–7.44 (m, 5H), 7.21 (td, J = 8.7, 5.8 Hz, 1H), 7.09–7.17 (m, 1H), 7.04 (dd, J = 7.8, 4.7 Hz, 1H), 4.48 (s, 2H).

8.3.29. *N*-(3-Amino-2,4-difluorophenyl)propane-2-sulfonamide (10h)

This material was prepared from **8** and propane-2-sulfonyl chloride according to the procedure described in Method A as light-yellow solid (0.760 g, 3.04 mmol, 32%). This compound was also prepared starting from **11** as described in Scheme 1. LCMS (ESI, pos. ion) calcd for $C_9H_{12}F_2N_2O_2S$: 250.1; found: 251.0 (M+1). ^{1}H NMR (400 MHz, $CDCl_3$) δ ppm 6.92 (dt, J = 5.5, 8.8 Hz, 1H), 6.74–6.84 (m, 1H), 6.29 (br s, 1H), 3.81 (br s, 2H), 3.27 (spt, J = 6.9 Hz, 1H), 1.40 (d, J = 6.8 Hz, 6H).

8.3.30. *N*-(3-(3-(9*H*-Purin-6-yl)pyridin-2-ylamino)-2,4-difluorophenyl)propane-2-sulfonamide (5h)[18a]

This compound was prepared from **12** and **10h** according to the sequence described for **4b** as an amorphous solid (0.583 g, 1.31 mmol, 43%). LCMS (ESI, pos. ion) calcd for $C_{19}H_{17}F_2N_7O_2S$: 445.1; found: 446.1 (M+1). ^{1}H NMR (400 MHz, DMSO-d_6) δ ppm 13.86 (br s, 1H), 11.56 (br s, 1H), 9.50–9.84 (m, 2H), 9.05 (s, 1H),

8.74 (s, 1H), 8.17–8.25 (m, 1H), 7.27–7.39 (m, 1H), 7.13–7.24 (m, 1H), 7.00–7.10 (m, 1H), 3.19–3.30 (m, 1H), 1.31 (d, *J* = 6.8 Hz, 6H).

8.3.31. *N*-(3-((3-(9*H*-Purin-6-yl)pyridin-2-yl)amino)-2,4-difluorophenyl)butane-2-sulfonamide (5i)

This compound was prepared from **14** and butane-2-sulfonyl chloride according to the procedure described in Method B as an amorphous solid (46 mg, 0.10 mmol, 34%). LCMS (ESI, pos. ion) calcd for $C_{20}H_{19}F_2N_7O_2S$: 459.1; found: 460.2 (M+1). ^{1}H NMR (400 MHz, DMSO-d_6) δ ppm 13.31–14.01 (m, 1H), 11.39 (br s, 1H), 9.52 (br s, 2H), 8.90 (s, 1H), 8.59 (s, 1H), 8.06 (d, *J* = 2.4 Hz, 1H), 7.18 (d, *J* = 5.7 Hz, 1H), 6.98–7.10 (m, 1H), 6.91 (dd, *J* = 4.7, 7.4 Hz, 1H), 2.87 (br s, 1H), 1.85 (d, *J* = 4.7 Hz, 1H), 1.25–1.47 (m, 1H), 1.17 (d, *J* = 6.6 Hz, 3H), 0.82 (t, *J* = 7.1 Hz, 3H).

8.3.32. *N*-(3-Amino-2,4-difluorophenyl)pentane-2-sulfonamide (10j)

This material was prepared from **8** and pentane-2-sulfonyl chloride according to the procedure described in Method A as colorless oil (30 mg, 0.11 mmol, 10%). LCMS (ESI, pos. ion) calcd for $C_{11}H_{16}F_2N_2O_2S$: 278.0; found: 279.0 (M+1). ^{1}H NMR (400 MHz, $CDCl_3$) δ ppm 6.92 (td, *J* = 8.9, 5.4 Hz, 1H), 6.74–6.85 (m, 1H), 6.25 (br s, 1H), 3.81 (br s, 2H), 3.10 (ddd, *J* = 9.9, 6.6, 3.4 Hz, 1H), 1.96 (ddd, *J* = 9.9, 6.6, 2.7 Hz, 1H), 1.59–1.66 (m, 1H), 1.45–1.54 (m, 1H), 1.38 (d, *J* = 6.8 Hz, 3H), 1.24–1.35 (m, 1H), 0.92 (t, *J* = 7.2 Hz, 3H).

8.3.33. *N*-(3-(3-(9*H*-Purin-6-yl)pyridin-2-ylamino)-2,4-difluorophenyl)pentane-2-sulfonamide (5j)

This compound was prepared from **10j** and **12** according to the sequence described for **4b** as an amorphous solid (15 mg, 0.032 mmol, 49%). LCMS (ESI, pos. ion) calcd for $C_{21}H_{21}F_2N_7O_2S$: 473.1; found: 474.0 (M+1). ^{1}H NMR (300 MHz, DMSO-d_6) δ ppm 11. 53 (br s, 1H), 9.67 (br s, 2H), 9.03 (s, 1H), 8.72 (s, 1H), 8.19 (dd, *J* = 4.7, 1.9 Hz, 1H), 7.30 (td, *J* = 8.8, 5.8 Hz, 1H), 7.09–7.22 (m, 1H), 7.03 (dd, *J* = 7.9, 4.8 Hz, 1H), 2.96–3.16 (m, 1H), 1.80–1.96 (m, 1H), 1.35–1.52 (m, 2H), 1.21–1.33 (m, 4H), 0.86 (t, *J* = 7.2 Hz, 3H).

8.3.34. *N*-(3-Amino-2,4-difluorophenyl)cyclopropanesulfonamide (10k)

This material was prepared from **8** and cyclopropanesulfonyl chloride according to the procedure described in Method A as yellow solid (0.278 g, 1.15 mmol, 68%). LCMS (ESI, pos. ion) calcd for $C_9H_{10}F_2N_2O_2S$: 248.0; found: 249.2 (M+1). ^{1}H NMR (400 MHz, DMSO-d_6) δ ppm 9.33 (s, 1H), 6.87 (ddd, *J* = 2.0, 8.9, 10.7 Hz, 1H), 6.54 (dt, *J* = 5.5, 8.6 Hz, 1H), 5.31 (s, 2H), 2.52–2.67 (m, 1H), 0.90–0.97 (m, 2H), 0.81–0.89 (m, 2H).

8.3.35. *N*-(3-(3-(9*H*-Purin-6-yl)pyridin-2-ylamino)-2,4-difluorophenyl)cyclopropanesulfonamide (5k)[18a]

This compound was prepared from **10k** and **12** according to the sequence described for **4b** as an amorphous solid (36 mg, 0.081 mmol, 16%). LCMS (ESI, pos. ion) calcd for $C_{19}H_{15}F_2N_7O_2S$: 443.1; found: 444.2 (M+1). ^{1}H NMR (400 MHz, DMSO-d_6) δ ppm 11.58 (br s, 1H), 9.66 (d, *J* = 6.2 Hz, 1H), 9.03 (s, 1H), 8.71 (s, 1H), 8.21 (dd, *J* = 1.8, 4.7 Hz, 1H), 7.31 (d, *J* = 6.0 Hz, 1H), 7.20 (t, *J* = 9.3 Hz, 1H), 7.04 (dd, *J* = 4.8, 7.8 Hz, 1H), 2.65 (s, 1H), 0.94–1.05 (m, 2H), 0.85–0.92 (m, 2H).

8.3.36. *N*-(3-(3-(9*H*-Purin-6-yl)pyridin-2-ylamino)-2,4-difluorophenyl)cyclobutanesulfonamide (5l)[18a]

This compound was prepared from **14** and cyclobutanesulfonyl chloride according to the procedure described in Method B as an amorphous solid (63.2 mg, 0.138 mmol, 46%). LCMS (ESI, pos. ion) calcd for $C_{20}H_{17}F_2N_7O_2S$: 457.1; found: 458.0 (M+1). ^{1}H NMR (500 MHz, DMSO-d_6) δ ppm 11.44–11.54 (m, 1H), 9.57–9.67 (m, 2H), 9.00–9.05 (m, 1H), 8.71 (s, 1H), 8.19 (dd, *J* = 4.7, 1.9 Hz, 1H), 7.32 (td, *J* = 8.9, 5.6 Hz, 1H), 7.09–7.21 (m, 1H), 6.97–7.07 (m, 1H), 4.19 (br s, 1H), 3.09 (d, *J* = 7.0 Hz, 2H), 1.05–1.12 (m, 1H), 0.54–0.59 (m, 2H), 0.33–0.40 (m, 2H).

8.3.37. *N*-(3-Amino-2,4-difluorophenyl)cyclopentanesulfonamide (10m)

This material was prepared from **8** and cyclopentanesulfonyl chloride according to the procedure described in Method A as yellow oil (64.0 mg, 0.232 mmol, 17%). LCMS (ESI, pos. ion) calcd for $C_{11}H_{14}F_2N_2O_2S$: 276.1; found: 277.2 (M+1).

8.3.38. *N*-(3-(3-(9*H*-Purin-6-yl)pyridin-2-ylamino)-2,4-difluorophenyl)cyclopentanesulfonamide (5m)

This compound was prepared from **10m** and **12** according to the sequence described for **4b** as an amorphous solid (59.0 mg, 0.125 mmol, 54%). LCMS (ESI, pos. ion) calcd for $C_{21}H_{19}F_2N_7O_2S$: 471.1; found: 472.2 (M+1). ^{1}H NMR (400 MHz, DMSO-d_6) δ ppm 11.44 (br s, 1H), 9.57 (br s, 2H), 8.96 (s, 1H), 8.64 (s, 1H), 8.12 (dd, *J* = 1.6, 4.6 Hz, 1H), 7.18–7.31 (m, 1H), 7.09 (t, *J* = 8.7 Hz, 1H), 6.96 (dd, *J* = 4.7, 7.8 Hz, 1H), 3.48 (t, *J* = 7.7 Hz, 1H), 1.77–1.95 (m, 4H), 1.59 (d, *J* = 6.6 Hz, 2H), 1.50 (d, *J* = 6.8 Hz, 2H).

8.3.39. *N*-(3-(3-(9*H*-Purin-6-yl)pyridin-2-ylamino)-2,4-difluorophenyl)tetrahydrofuran-3-sulfonamide (5n)

This compound was prepared from **14** and tetrahydrofuran-3-sulfonyl chloride according to the procedure described in Method B as an amorphous solid (39 mg, 0.082 mmol, 54%). LCMS (ESI, pos. ion) calcd for $C_{20}H_{17}F_2N_7O_3S$: 473.1; found: 474.0 (M+1). ^{1}H NMR (400 MHz, DMSO-d_6) δ ppm 11.60 (br s, 1H), 9.72 (br s, 1H), 9.09 (s, 1H), 8.78 (s, 1H), 8.26 (dd, *J* = 1.8, 4.7 Hz, 1H), 7.36 (dt, *J* = 6.0, 8.6 Hz, 1H), 7.17–7.29 (m, 1H), 7.10 (dd, *J* = 4.7, 7.8 Hz, 1H), 4.02–4.09 (m, 1H), 3.95–4.02 (m, 2H), 3.83–3.94 (m, 1H), 3.67–3.82 (m, 1H), 2.16–2.34 (m, 2H).

8.3.40. *N*-(3-Amino-2,4-difluorophenyl)cyclohexanesulfonamide (10o)

This material was prepared from **8** and cyclohexanesulfonyl chloride according to the procedure described in Method A as a white solid (0.161 g, 0.555 mmol, 34%). LCMS (ESI, pos. ion) calcd for $C_{12}H_{16}F_2N_2O_2S$: 290.1; found: 291.1 (M+1). ^{1}H NMR (400 MHz, DMSO-d_6) δ ppm 9.34 (br s, 1H), 6.78–6.94 (m, 1H), 6.53 (dt, *J* = 5.5, 8.7 Hz, 1H), 5.31 (s, 2H), 2.81–2.95 (m, 1H), 2.02–2.16 (m, 2H), 1.72–1.82 (m, 2H), 1.61 (d, *J* = 11.8 Hz, 1H), 1.32–1.48 (m, 2H), 1.17–1.31 (m, 2H), 1.09–1.15 (m, 1H).

8.3.41. *N*-(3-(3-(9*H*-Purin-6-yl)pyridin-2-ylamino)-2,4-difluorophenyl)cyclohexanesulfonamide (5o)

This compound was prepared from **10o** and **12** according to the sequence described for **4b** as an amorphous solid (0.117 g, 0.241 mmol, 53%). LCMS (ESI, pos. ion) calcd for $C_{22}H_{21}F_2N_7O_2S$: 485.1; found: 486.2 (M+1). ^{1}H NMR (400 MHz, DMSO-d_6) δ ppm 13.72–14.00 (m, 1H), 11.57 (br s, 1H), 9.52–9.85 (m, 2H), 9.03 (s, 1H), 8.73 (s, 1H), 8.20 (dd, *J* = 2.0, 4.8 Hz, 1H), 7.31 (dt, *J* = 5.7, 8.8 Hz, 1H), 7.13–7.23 (m, 1H), 7.04 (dd, *J* = 4.7, 7.9 Hz, 1H), 2.96 (t, *J* = 11.8 Hz, 1H), 2.11 (d, *J* = 11.6 Hz, 2H), 1.79 (d, *J* = 13.5 Hz, 2H), 1.55–1.70 (m, 1H), 1.34–1.49 (m, 2H), 1.18–1.32 (m, 2H), 1.13 (d, *J* = 11.7 Hz, 1H).

8.3.42. *N*-(3-((3-(9*H*-Purin-6-yl)pyridin-2-yl)amino)-2,4-difluorophenyl)tetrahydro-2*H*-pyran-4-sulfonamide (5p)

This compound was prepared from **14** and tetrahydro-2*H*-pyran-4-sulfonyl chloride according to the procedure described in Method B as an amorphous solid (21.7 mg, 0.045 mmol, 15%). LCMS (ESI, pos. ion) calcd for $C_{21}H_{19}F_2N_7O_3S$: 487.1; found: 488.0 (M+1). ^{1}H NMR (500 MHz, DMSO-d_6) δ ppm 9.69 (s, 1H),

7.15–7.19 (m, 1H), 7.01–7.08 (m, 1H), 4.08 (br s, 1H), 3.87–4.01 (m, 5H), 3.80 (s, 3H), 3.82 (s, 3H), 3.67 (d, J = 10.7 Hz, 2H), 3.39 (d, J = 11.5 Hz, 1H), 1.93–2.04 (m, 1H), 1.64–1.76 (m, 1H).

8.3.43. *N*-(3-Amino-2,4-difluorophenyl)-*N*,*N*-dimethylsulfamide (16a)

8.3.43.1. (a) *tert*-Butyl 3-(*N*,*N*-dimethylsulfamoyl)-2,6-difluorophenylcarbamate. To a solution of *tert*-butyl 3-amino-2,6-difluorophenylcarbamate[34] (**15**, 0.600 g, 2.46 mmol) in pyridine (10.0 mL) was added dimethylamine (1.60 mL, 3.19 mmol) and *N*,*N*-dimethylpyridin-4-amine (0.075 g, 0.614 mmol). The reaction mixture was cooled to −30 °C and stirred for 10 min before sulfuryl dichloride (0.299 mL, 3.68 mmol) was added dropwise. After an additional 20 min, the mixture was allowed to warm to rt. The reaction mixture was poured into EtOAc (30 mL) and vigorously stirred for 10 min. The EtOAc layer was separated. The tarry residue was triturated with DCM (3 mL) and EtOAc (20 ml). The combined organic layers were concentrated in vacuo. The crude product was purified by column chromatography using MeOH in DCM (3–5%) to afford the desired product (0.500 g, 1.42 mmol, 58%) as light-brown solid. LCMS (ESI, pos. ion) calcd for $C_{13}H_{19}F_2N_3O_4S$: 351.1; found: 374.0 (M+Na). ^{1}H NMR (300 MHz, $CDCl_3$) δ ppm 7.42 (td, J = 8.9, 5.5 Hz, 1H), 6.87–7.00 (m, 1H), 6.33 (br s, 1H), 5.97 (br s, 1H), 2.84 (s, 6H), 1.52 (s, 9H).

8.3.43.2. (b) *N*-(3-Amino-2,4-difluorophenyl)-*N*,*N*-dimethylsulfamide (16a). To a solution of *tert*-butyl 3-(*N*,*N*-dimethylsulfamoyl)-2,6-difluorophenylcarbamate (0.500 g, 1.42 mmol) in DCM (5.0 mL) was added trifluoroacetic acid (2.11 mL, 28.5 mmol). The resulting mixture was capped and stirred at rt for 2 h. The reaction mixture was neutralized using NaOH (aq, 5 N). The aqueous layer was extracted with DCM. The combined organic layers were dried over $MgSO_4$, filtered, and concentrated. The crude product was purified by column chromatography using MeOH in DCM (3–8%) to obtain the desired product (0.240 g, 0.955 mmol, 67%) as yellow solid. LCMS (ESI, pos. ion) calcd for $C_8H_{11}F_2N_3O_2S$: 251.2; found: 252.1 (M+1). ^{1}H NMR (300 MHz, $CDCl_3$) δ ppm 6.84–6.94 (m, 1H), 6.75–6.84 (m, 1H), 6.28 (br s, 1H), 3.80 (br s, 2H), 2.77–2.90 (m, 6H).

8.3.44. *N*-(3-(3-(9*H*-Purin-6-yl)pyridin-2-ylamino)-2,4-difluorophenyl)-*N*,*N*-dimethylsulfamide (6a)

8.3.44.1. (a) *N*-(2,4-Difluoro-3-(3-(9-(tetrahydro-2*H*-pyran-2-yl)-9*H*-purin-6-yl)pyridin-2-ylamino)-*N*,*N*-dimethylsulfamide.

To a solution of 6-(2-fluoropyridin-3-yl)-9-(tetrahydro-2*H*-pyran-2-yl)-9*H*-purine (**12**, 0.120 g, 0.400 mmol) and *N*-(3-amino-2,4-difluorophenyl)-*N*,*N*-dimethylsulfamide (**16a**, 0.121 g, 0.480 mmol) in THF (5.0 mL) was added sodium bis(trimethylsilyl)amide (1.0 M in THF, 1.60 mL, 1.60 mmol) at 0 °C in one portion. The dark-red mixture was stirred at 0 °C for 10 min and at rt for 30 min. The reaction mixture was partitioned between EtOAc and a buffer solution (sodium citrate, pH 5). The aqueous layer was extracted with EtOAc. The combined organic layers were dried over $MgSO_4$, filtered, and concentrated. The crude product was purified by column chromatography using acetone in hexane (20–30%) to afford the THP-protected product (0.145 g, 0.273 mmol, 68%) as a yellow solid. LCMS (ESI, pos. ion) calcd for $C_{23}H_{24}F_2N_8O_3S$: 530.2; found: 531.2 (M+1).

8.3.44.2. (b) *N*-(3-(3-(9*H*-Purin-6-yl)pyridin-2-ylamino)-2,4-difluorophenyl)-*N*,*N*-dimethylsulfamide (6a). To a solution of *N*-(2,4-difluoro-3-(3-(9-(tetrahydro-2*H*-pyran-2-yl)-9*H*-purin-6-yl)pyridin-2-ylamino)-*N*,*N*-dimethylsulfamide (0.145 g, 0.270 mmol) in THF (2.0 mL) was added hydrogen chloride (aq, 5 N, 1.09 mL, 5.47 mmol). The resulting mixture was stirred at rt in a closed system for 1 h. The mixture was partitioned between a buffer solution (pH ~7) and $CHCl_3$. The aqueous layer was extracted with $CHCl_3$. The combined organic layers were dried over $MgSO_4$, filtered, and concentrated. The crude product was purified by column chromatography using MeOH in DCM (3–8%) to obtain the desired product (0.105 g, 0.235 mmol, 85%) as yellow solid. LCMS (ESI, pos. ion) calcd for $C_{18}H_{16}F_2N_8O_2S$: 446.1; found: 447.0 (M+1). ^{1}H NMR (300 MHz, DMSO-d_6) δ ppm 11.55 (br s, 1H), 9.69 (d, J = 7.4 Hz, 1H), 9.58 (br s, 1H), 9.04 (s, 1H), 8.72 (s, 1H), 8.19 (dd, J = 4.8, 1.8 Hz, 1H), 7.32 (td, J = 8.7, 5.8 Hz, 1H), 7.11–7.22 (m, 1H), 7.03 (dd, J = 7.8, 4.8 Hz, 1H), 2.73 (s, 6H).

8.3.45. *N*-(3-Amino-2,4-difluorophenyl)-*N*-ethyl-*N*-methylsulfamide (16b)

8.3.45.1. (a) *N*-(3-(*N*-Ethyl-*N*-methylsulfamoylamino)-2,6-difluorophenyl)acetamide. To a solution of *N*-(3-amino-2,6-difluorophenyl)acetamide (**8**, 0.500 g, 2.69 mmol) in pyridine (10.0 mL) was added *N*,*N*-dimethylpyridin-4-amine (0.082 g, 0.67 mmol) and *N*-ethylmethylamine (0.300 mL, 3.49 mmol) under N_2. The reaction mixture was cooled to −30 °C and stirred for 10 min before sulfuryl chloride (0.327 mL, 4.03 mmol) was added dropwise. After 20 min, the mixture was allowed to warm to rt and continued to stir for 1 h. The reaction mixture was poured into with EtOAc (30 mL) and vigorously stirred for 10 min. The EtOAc layer was separated. The tarry residue was dissolved in DCM (3 mL) followed by addition of EtOAc (20 mL). This mixture was vigorously stirred for 10 min and the organic layer was decanted. The combined organic layers were concentrated and the crude product was purified by column chromatography using acetone in hexanes (10–40%) to obtain the desired product (0.400 g, 1.30 mmol, 49%) as yellow solid. LCMS (ESI, pos. ion) calcd for $C_{11}H_{15}F_2N_3O_3S$: 307.1; found: 308.0 (M+1). ^{1}H NMR (300 MHz, $CDCl_3$) δ ppm 7.45 (td, J = 8.8, 5.6 Hz, 1H), 6.96 (td, J = 9.1, 2.0 Hz, 1H), 6.75 (br s, 1H), 6.36 (br s, 1H), 3.22 (q, J = 7.1 Hz, 2H), 2.83 (s, 3H), 2.16–2.32 (m, 3H), 1.11 (t, J = 7.09 Hz, 3H).

8.3.45.2. (b) *N*-(3-Amino-2,4-difluorophenyl)-*N*-ethyl-*N*-methylsulfamide (16b). To a 20-mL microwave vial was added *N*-(3-(*N*-ethyl-*N*-methylsulfamoylamino)-2,6-difluorophenyl)acetamide (0.400 g, 1.30 mmol), concentrated HCl (1.60 mL, 19.5 mmol), and EtOH (10.0 mL). The vial was capped and heated at 90 °C for 4 h. The reaction mixture was concentrated and the residue was partitioned between EtOAc and saturated sodium bicarbonate. The aqueous layer was extracted with EtOAc. The combined organic layers were dried over $MgSO_4$, filtered, and concentrated. The crude product was purified by column chromatography using acetone in hexanes (10–30%) to afford the desired product (0.275 g, 1.04 mmol, 80%) as a white solid. LCMS (ESI, pos. ion) calcd for $C_9H_{13}F_2N_3O_2S$: 265.1; found: 266.0 (M+1). ^{1}H NMR (300 MHz, $CDCl_3$) δ ppm 6.69–6.95 (m, 2H), 6.29 (br s, 1H), 3.79 (br s, 2H), 3.22 (q, J = 7.2 Hz, 2H), 2.83 (s, 3H), 1.11 (t, J = 7.2 Hz, 3H).

8.3.46. *N*-(3-(3-(9*H*-Purin-6-yl)pyridin-2-ylamino)-2,4-difluorophenyl)-*N*-ethyl-*N*-methylsulfamide (6b)

This material was prepared in a similar procedure as described for **6a** as an amorphous solid (0.080 g, 0.17 mmol, 79%). LCMS (ESI, pos. ion) calcd for $C_{19}H_{18}F_2N_8O_2S$: 460.1; found: 461.0 (M+1). ^{1}H NMR (300 MHz, DMSO-d_6) δ ppm 11.54 (s, 1H), 9.69 (d, J = 6.7 Hz, 1H), 9.54 (br s, 1H), 9.04 (s, 1H), 8.72 (s, 1H), 8.19 (dd, J = 4.8, 1.8 Hz, 1H), 7.30 (td, J = 8.8, 5.8 Hz, 1H), 7.11–7.22 (m, 1H), 7.03 (dd, J = 7.8, 4.8 Hz, 1H), 3.11 (q, J = 7.2 Hz, 2H), 2.73 (s, 3H), 1.03 (t, J = 7.2 Hz, 3H).

8.3.47. *N*-(3-(3-(9*H*-Purin-6-yl)pyridin-2-ylamino)-2,4-difluorophenyl)-*N*,*N*-diethylsulfamide (6c)

A pressure-resistant vial was charged with 2,6-difluoro-*N*1-(3-(9-(tetrahydro-2*H*-pyran-2-yl)-9*H*-purin-6-yl)pyridin-2-yl)benzene-1,3-diamine (**14**, 0.140 g, 0.33 mmol), pyridine (80 μL, 0.99 mmol),

DCM (3.3 mL), and diethylsulfamoyl chloride (0.80 mL, 4.65 mmol). The mixture was heated at 60 °C for 2 d. The mixture was cooled to rt and was diluted with DCM and water. The organic layer was concentrated and the residue was suspended in HCl (aq, 6 N, 0.280 mL, 1.65 mmol) and THF (3.3 mL). The resulting mixture was stirred at rt for 1 h and concentrated under reduced pressure to afford a yellow residue. The resulting crude product was purified by HPLC (10–70% CH_3CN/H_2O; 0.1% TFA) to afford the desired product as TFA salt (0.015 g, 0.025 mmol, 7.7%). LCMS (ESI, pos. ion) calcd for $C_{20}H_{20}F_2N_8O_2S$: 474.1; found: 475.2 (M+1). ^{1}H NMR (400 MHz, DMSO-d_6) δ ppm 11.50 (br s, 1H), 9.64 (br s, 1H), 9.49 (s, 1H), 9.05 (s, 1H), 8.73 (s, 1H), 8.20 (dd, J = 1.9, 4.7 Hz, 1H), 7.30 (d, J = 5.9 Hz, 1H), 7.18 (t, J = 9.2 Hz, 1H), 7.04 (dd, J = 4.7, 7.9 Hz, 1H), 3.18 (q, J = 7.1 Hz, 4H), 1.03 (t, J = 7.1 Hz, 6H).

8.3.48. *N*-(3-(3-(9*H*-Purin-6-yl)pyridin-2-ylamino)-2,4-difluorophenyl)pyrrolidine-1-sulfonamide (6d)

8.3.48.1. (a) *N*-(2,4-Difluoro-3-(3-(9-(tetrahydro-2*H*-pyran-2-yl)-9*H*-purin-6-yl)pyridin-2-ylamino)phenyl)pyrrolidine-1-sulfonamide. To a solution of 2,6-difluoro-*N*1-(3-(9-(tetrahydro-2*H*-pyran-2-yl)-9*H*-purin-6-yl)pyridin-2-yl)benzene-1,3-diamine (**14**, 0.150 g, 0.35 mmol) in pyridine (5.0 mL) was added 4-(dimethylamino)pyridine (0.022 g, 0.18 mmol) and pyrrolidine (0.039 mL, 0.46 mmol). The reaction mixture was cooled to −30 °C and was stirred for 10 min. Sulfuryl chloride (0.043 mL, 0.53 mmol) was added dropwise. After the addition, the mixture was allowed to stir for an additional 20 min before it was stirred at rt for 1 h. The reaction mixture was poured into EtOAc (20 ml) and stirred for 10 min. The organic layer was separated and the residue was dissolved into DCM (3 mL) followed by addition of EtOAc (20 mL). The mixture was stirred for 10 min and the organic layer was separated. The combined organic layers were concentrated and the crude product was purified by column chromatography using DCM/EtOAc/MeOH (70%/27%/3%) to obtain the desired product (0.090 g, 0.16 mmol, 46%) as yellow solid. LCMS (ESI, pos. ion) calcd for $C_{25}H_{26}F_2N_8O_3S$: 556.2; found: 556.8 (M+1). ^{1}H NMR (300 MHz, $CDCl_3$) δ ppm 11.58 (s, 1H), 9.66 (dd, J = 7.9, 1.8 Hz, 1H), 9.02 (s, 1H), 8.39 (s, 1H), 8.23 (dd, J = 4.7, 1.9 Hz, 1H), 7.45 (td, J = 8.8, 5.4 Hz, 1H), 6.84–7.09 (m, 2H), 6.47 (s, 1H), 5.90 (dd, J = 10.2, 2.5 Hz, 1H), 4.16–4.32 (m, 1H), 3.84 (td, J = 11.7, 2.6 Hz, 1H), 3.20–3.45 (m, 4H), 2.06–2.27 (m, 3H), 1.67–1.95 (m, 7H).

8.3.48.2. (b) *N*-(3-(3-(9*H*-Purin-6-yl)pyridin-2-ylamino)-2,4-difluorophenyl)pyrrolidine-1-sulfonamide (6d). To a solution of *N*-(2,4-difluoro-3-(3-(9-(tetrahydro-2*H*-pyran-2-yl)-9*H*-purin-6-yl)pyridin-2-ylamino)phenyl)pyrrolidine-1-sulfonamide (0.080 g, 0.14 mmol) in THF (2.0 mL) was added HCl (aq, 5 N, 0.575 mL, 2.87 mmol). The resulting mixture was stirred at rt for 2 h. The mixture was partitioned between a buffer solution (KH_2PO_4–Na_2HPO_4, pH 7) and $CHCl_3$. The aqueous layer was extracted with $CHCl_3$. The combined organic layers were dried over $MgSO_4$, filtered, and concentrated. The crude product was purified by column chromatography using MeOH in DCM (3–6%) to afford the **6d** (0.0550 g, 0.116 mmol, 81%) as a yellow solid. LCMS (ESI, pos. ion) calcd for $C_{20}H_{18}F_2N_8O_2S$: 472.1; found: 473.0 (M+1). ^{1}H NMR (300 MHz, DMSO-d_6) δ ppm 11.52 (br s, 1H), 9.65 (br s, 2H), 9.04 (s, 1H), 8.73 (s, 1H), 8.18 (dd, J = 4.7, 1.9 Hz, 1H), 7.35 (td, J = 8.8, 5.7 Hz, 1H), 7.17 (td, J = 9.2, 1.6 Hz, 1H), 7.04 (dd, J = 7.8, 4.8 Hz, 1H), 3.09–3.26 (m, 4H), 1.64–1.90 (m, 4H).

8.3.49. *N*-(3-Amino-2,4-difluorophenyl)piperidine-1-sulfonamide (16e)

This compound was prepared from **8** and piperidine according to the sequence described for **16b** as a white solid (0.275 g, 0.944 mmol, 35%). LCMS (ESI, pos. ion) calcd for $C_{11}H_{15}F_2N_3O_2S$: 291.1; found: 292.1 (M+1). ^{1}H NMR (300 MHz, $CDCl_3$) δ ppm 6.68–6.97 (m, 2H), 6.27 (br s, 1H), 3.79 (br s, 2H), 3.13–3.27 (m, 4H), 1.49–1.63 (m, 6H).

8.3.50. *N*-(3-(3-(9*H*-Purin-6-yl)pyridin-2-ylamino)-2,4-difluorophenyl)piperidine-1-sulfonamide (6e)

This compound was prepared from **16e** and **12** according to the sequence described for **6a** as an amorphous solid (95 mg, 0.20 mmol, 50%). LCMS (ESI, pos. ion) calcd for $C_{21}H_{20}F_2N_8O_2S$: 486.1; found: 487.1 (M+1). ^{1}H NMR (300 MHz, DMSO-d_6) δ ppm 11.52 (br s, 1H), 9.66 (br s, 2H), 9.03 (s, 1H), 8.72 (s, 1H), 8.18 (dd, J = 4.8, 1.8 Hz, 1H), 7.32 (td, J = 8.8, 5.8 Hz, 1H), 7.16 (td, J = 9.3, 1.6 Hz, 1H), 7.03 (dd, J = 7.8, 4.8 Hz, 1H), 3.09 (d, J = 5.3 Hz, 4H), 1.48 (d, J = 4.7 Hz, 6H).

8.3.51. *N*-(2,4-Difluoro-3-(3-(9-(tetrahydro-2*H*-pyran-2-yl)-9*H*-purin-6-yl)pyridin-2-ylamino)phenyl)-2-oxooxazolidine-3-sulfonamide (17)

To a mixture of chlorosulfonyl isocyanate (0.154 mL, 1.77 mmol) in DCM (5.89 mL) cooled at 0 °C under N_2 was added 2-bromoethanol (0.125 mL, 1.77 mmol). After 1 h, a suspension of 2,6-difluoro-*N*1-(3-(9-(tetrahydro-2*H*-pyran-2-yl)-9*H*-purin-6-yl) pyridin-2-yl)benzene-1,3-diamine (**14**, 0.748 g, 1.77 mmol) and triethylamine (0.492 mL, 3.53 mmol) in DCM (6 mL) was added dropwise. The resulting yellow suspension was stirred at 0 °C for 20 min and at rt for 1 h. The solution was cooled to 0 °C and was quenched with HCl (aq, 10%, 3.5 mL) followed by DCM (20 mL). The layers were separated and the organic layer was washed with water, dried over sodium sulfate, filtered, and concentrated to afford **17** (0.900 g, 1.57 mmol, 89%) as a yellow solid. LCMS (ESI, pos. ion) calcd for $C_{24}H_{22}F_2N_8O_5S$: 572.1; found: 573.2 (M+1).

8.3.52. (3*S*)-*N*-(3-(3-(9*H*-Purin-6-yl)pyridin-2-ylamino)-2,4-difluorophenyl)-3-hydroxypyrrolidine-1-sulfonamide (6f)

8.3.52.1. (a) (3*S*)-*N*-(2,4-Difluoro-3-(3-(9-(tetrahydro-2*H*-pyran-2-yl)-9*H*-purin-6-yl)pyridin-2-ylamino)phenyl)-3-hydroxypyrrolidine-1-sulfonamide. To a suspension of *N*-(2,4-difluoro-3-(3-(9-(tetrahydro-2*H*-pyran-2-yl)-9*H*-purin-6-yl)pyridin-2-ylamino)phenyl)-2-oxooxazolidine-3-sulfonamide (**17**, 0.340 g, 0.590 mmol) in acetonitrile (1.2 mL) was added 4Å molecular sieves and (*S*)-pyrrolidin-3-ol (0.480 mL, 5.94 mmol) followed by triethylamine (0.858 mL, 5.94 mmol). After being stirred at 110 °C overnight, the reaction mixture was allowed to cool to rt and was diluted with DCM. The suspension was filtered, and the residue was rinsed with MeOH in DCM (10%). The combined filtrates were concentrated and purified on silica gel with MeOH in DCM (2%) to afford the product (0.035 g, 0.061 mmol, 10%). LCMS (ESI, pos. ion) calcd for $C_{25}H_{26}F_2N_8O_4S$: 572.2; found: 573.2 (M+1).

8.3.52.2. (b) (3*S*)-*N*-(3-(3-(9*H*-Purin-6-yl)pyridin-2-ylamino)-2,4-difluorophenyl)-3-hydroxypyrrolidine-1-sulfonamide hydrochloride (6f). To a suspension of (3*S*)-*N*-(2,4-difluoro-3-(3-(9-(tetrahydro-2*H*-pyran-2-yl)-9*H*-purin-6-yl)pyridin-2-ylamino) phenyl)-3-hydroxypyrrolidine-1-sulfonamide (0.030 g, 0.052 mmol) in THF (0.21 mL) was added HCl (aq, 6 N, 0.044 mL, 0.26 mmol). After being stirred at rt for 2 h, the mixture was concentrated to dryness and the residue was triturated with acetonitrile. The solids were collected and was dried under high vacuum to afford (3*S*)-*N*-(3-(3-(9*H*-purin-6-yl)pyridin-2-ylamino)-2,4-difluorophenyl)-3-hydroxypyrrolidine-1-sulfonamide hydrochloride as an amorphous solid (**6f**, 15 mg, 0.029 mmol, 54%). LCMS (ESI, pos. ion) calcd for $C_{20}H_{18}F_2N_8O_3S$: 488.1; found: 489.2 (M+1). ^{1}H NMR (400 MHz, DMSO-d_6) δ ppm 11.53 (s, 1H), 9.65 (d, J = 6.2 Hz, 1H), 9.52 (s, 1H), 9.04 (s, 1H), 8.73 (s, 1H), 8.21 (dd, J = 1.9, 4.8 Hz, 1H), 7.36 (dt, J = 5.7, 8.8 Hz, 1H), 7.10–7.23 (m, 1H), 7.05 (dd, J = 4.7, 7.9 Hz, 1H),

4.24–4.37 (m, 1H), 3.23–3.39 (m, 3H), 3.06 (dd, J = 2.2, 9.9 Hz, 1H), 1.85–2.00 (m, 1H), 1.68–1.81 (m, 1H).

8.3.53. (3*R*)-*N*-(3-(3-(9*H*-Purin-6-yl)pyridin-2-ylamino)-2,4-difluorophenyl)-3-hydroxypyrrolidine-1-sulfonamide (6g)

This compound was prepared from (*R*)-pyrrolidin-3-ol according to the procedure described for **6f** as an amorphous solid (HCl salt, 15 mg, 0.029 mmol, 63%). LCMS (ESI, pos. ion) calcd for $C_{20}H_{18}F_2N_8O_3S$: 488.1; found: 489.2 (M+1). ^{1}H NMR (400 MHz, DMSO-d_6) δ ppm 11.57 (br s, 1H), 9.70 (d, J = 7.4 Hz, 1H), 9.57 (s, 1H), 9.09 (s, 1H), 8.78 (s, 1H), 8.26 (dd, J = 1.9, 4.7 Hz, 1H), 7.41 (dt, J = 5.7, 8.7 Hz, 1H), 7.21 (dt, J = 1.5, 9.2 Hz, 1H), 7.09 (dd, J = 4.7, 7.8 Hz, 1H), 4.29–4.41 (m, 1H), 3.28–3.45 (m, 3H), 3.11 (dd, J = 2.1, 10.0 Hz, 1H), 1.91–2.04 (m, 1H), 1.73–1.87 (m, 1H).

8.3.54. *N*-(3-Amino-2,4-difluorophenyl)morpholine-4-sulfonamide (16h)

8.3.54.1. (a) *tert*-Butyl 2,6-difluoro-3-(morpholine-4-sulfonamido)phenylcarbamate. To a solution of *tert*-butyl 3-amino-2,6-difluorophenylcarbamate (**15**, 0.600 g, 2.457 mmol) in pyridine (10.0 mL) was added 4-(dimethylamino)-pyridine (0.075 g, 0.614 mmol) and morpholine (0.278 mL, 3.19 mmol). The reaction mixture was cooled to −30 °C and sulfuryl chloride (0.299 mL, 3.68 mmol) was added dropwise. After the addition, the mixture was allowed to stir for an additional 20 min and then at rt for 2 h. The mixture was poured into cold EtOAc (30 mL) and was vigorously stirred for 10 min. The organic layer was decanted and the dark residue was dissolved in DCM (3 mL) followed by dilution with EtOAc (20 mL). The combined organic layers were concentrated in vacuo and the crude product was purified by column chromatography using NH_3–MeOH (2 N) in DCM (3–5%) to give the desired product as light-brown solid (730 mg, 1.85 mmol, 76%). LCMS (ESI, pos. ion) calcd for $C_{15}H_{21}F_2N_3O_5S$: 393.1; found: 416.0 (M+Na).

8.3.54.2. (b) *N*-(3-Amino-2,4-difluorophenyl)morpholine-4-sulfonamide (16h). To a 100-mL round-bottomed flask, *tert*-butyl 2,6-difluoro-3-(morpholine-4-sulfonamido)phenylcarbamate (0.496 g, 1.261 mmol) and TFA (5.0 mL, 64.9 mmol) were mixed in DCM (5 mL). The dark mixture was stirred at rt for 30 min and was neutralized with sodium bicarbonate to pH ~7. The mixture was extracted with DCM and 10% IPA/$CHCl_3$. The combined organic phases were dried over sodium sulfate, filtered, and concentrated. The crude product was purified on silica with EtOAc in hexanes (10–80%) to afford **16h** as light-brown film (150 mg, 0.511 mmol, 41%). LCMS (ESI, pos. ion) calcd for $C_{10}H_{13}F_2N_3O_3S$: 293.1; found: 294.0 (M+1). ^{1}H NMR (400 MHz, $CDCl_3$) δ ppm 6.75–6.94 (m, 2H), 6.28 (br s, 1H), 3.82 (br s, 2H), 3.62–3.73 (m, 4H), 3.17–3.29 (m, 4H).

8.3.55. *N*-(3-(3-(9*H*-Purin-6-yl)pyridin-2-ylamino)-2,4-difluorophenyl)morpholine-4-sulfonamide (6h)

This compound was prepared from **16h** and **12** according to the procedure described for **6a** as an amorphous solid (47 mg, 0.097 mmol, 20%). LCMS (ESI, pos. ion) calcd for $C_{20}H_{18}F_2N_8O_3S$: 488.1; found: 489.1 (M+1). ^{1}H NMR (400 MHz, DMSO-d_6) δ ppm 11.56 (br s, 1H), 9.68 (br s, 2H), 9.04 (s, 1H), 8.73 (s, 1H), 8.21 (d, J = 3.5 Hz, 1H), 7.13–7.42 (m, 2H), 7.04 (dd, J = 7.4, 4.9 Hz, 1H), 3.60 (br s, 4H), 3.10 (br s, 4H).

8.3.56. *N*-(3-(3-(9*H*-Purin-6-yl)pyridin-2-ylamino)-2,4-difluorophenyl)piperazine-1-sulfonamide (6i)

This compound was prepared from *tert*-butyl piperazine-1-carboxylate and **14** according to the procedure described for **6d** as an amorphous solid (68 mg, 0.139 mmol, 30%). LCMS (ESI, pos. ion) calcd for $C_{20}H_{19}F_2N_9O_2S$: 487.1; found: 488.1 (M+1). ^{1}H NMR (300 MHz, DMSO-d_6) δ ppm 11.61 (br s, 1H), 9.96 (br s, 1H), 9.69 (d, J = 7.2 Hz, 1H), 9.04 (s, 1H), 8.73 (s, 2H), 8.22 (dd, J = 4.8, 1.8 Hz, 1H), 7.33 (td, J = 8.7, 5.8 Hz, 1H), 7.13–7.25 (m, 1H), 7.05 (dd, J = 7.8, 4.8 Hz, 1H), 3.34 (br s, 4H, overlapping with water), 3.17 (br s, 4H).

Abbreviations

MAPK, mitogen activated protein kinases; ERK, extracellular signal-regulated kinases; ^{b}S, biochemical selectivity; ^{c}S, cellular selectivity; ^{p}A, percent of ERK activation as measured by the formation of phospho ERK (p-ERK); SAR, structure–activity relationship; ATP, adenosine-5′-triphosphate. Abbreviations for chemical reagents and experimental descriptions are adopted from the convention of the Journal of Organic Chemistry.

Acknowledgements

We thank Yunxin Bo, Debbie Choquette, Fang-Tsao Hong, Roxanne Kunz, Markian Stec, Seifu Tadesse, Nuria Tamayo, and Yong-Jae Kim for providing synthetic intermediates and for contributing to studies (unpublished) that extended the scope of the current series; Gina Ranieri, Richard Walter, and the staff of Shamrock Structures LLC for performing X-ray data collection. We also acknowledge Randy Hungate, Rick Kendall, and Philip Tagari for supporting this project and Margaret Chu-Moyer for providing helpful suggestions regarding the preparation of this manuscript.

Supplementary data

Supplementary data associated with this article can be found, in the online version, at http://dx.doi.org/10.1016/j.bmc.2016.03.055.

References and notes

1. For a review, see Sebolt-Leopold, J. S.; Herrera, R. *Nat. Rev. Cancer* **2004**, *4*, 937.
2. Davies, H.; Bignell, G. R.; Cox, C.; Stephens, P.; Edkins, S.; Clegg, S.; Teague, J.; Woffendin, H.; Garnett, M. J.; Bottomley, W.; Davis, N.; Dicks, E.; Ewing, R.; Floyd, Y.; Gray, K.; Hall, S.; Hawes, R.; Hughes, J.; Kosmidou, V.; Menzies, A.; Mould, C.; Parker, A.; Stevens, C.; Watt, S.; Hooper, S.; Wilson, R.; Jayatilake, H.; Gusterson, B. A.; Cooper, C.; Shipley, J.; Hargrave, D.; Pritchard- Jones, K.; Maitland, N.; Chenevix-Trench, G.; Riggins, G. J.; Bigner, D. D.; Palmieri, G.; Cossu, A.; Flanagan, A.; Nicholson, A.; Ho, J. W. C.; Leung, S. Y.; Yuen, S. T.; Weber, B. L.; Seigler, H. F.; Darrow, T. L.; Paterson, H.; Marais, R.; Marshall, C. J.; Wooster, R.; Stratton, M. R.; Futreal, P. A. *Nature* **2002**, *417*, 949; (b) Pollock, P. M.; Harper, U. L.; Hansen, K. S.; Yudt, LM.; Stark, M.; Robbins, C. M.; Moses, T. Y.; Hostetter, G.; Wagner, U.; Kakareka, J.; Salem, G.; Pohida, T.; Heenan, P.; Duray, P.; Kalioniemi, O.; Hayward, N. K.; Trent, J. M.; Meltzer, P. S. *Nat. Genet.* **2003**, *33*, 19.
3. Wan, P. T.; Garnett, M. J.; Roe, S. M.; Lee, S.; Niculescu-Duvaz, D.; Good, V. M.; Jones, C. M.; Marshall, C. J.; Springer, C. J.; Barford, D.; Marais, R. *Cell* **2004**, *116*, 855.
4. (a) Azjili, K.; Stelloo, E.; Peters, Godefridus. J.; van den Eertwrgh, A. J. M. *Anticancer Res.* **2014**, *34*, 1493; (b) Gray-Schopfer, V.; Wellbrock, C.; Marais, R. *Nature* **2007**, *445*, 852.
5. (a) Wilhelm, S. M.; Carter, C.; Tang, L.; Wilkie, D.; McNabola, A.; Rong, H.; Chen, C.; Zhang, X.; Vincent, P.; McHugh, M.; Cao, Y.; Shujath, J.; Gawlak, S.; Eveleigh, D.; Rowley, B.; Liu, L.; Adnane, L.; Lynch, M.; Auclair, D.; Taylor, I.; Gedrich, R.; Voznesensky, A.; Riedl, B.; Post, L. E.; Bollag, G. *Cancer Res.* **2004**, *64*, 7099; For recent examples of this type of compounds with improved selectivity, see, (b) Zambon, A.; Menard, D.; Suijkerbuijk, B. M. J. M.; Niculescu-Duvaz, I.; Whittaker, S.; Niculescu-Duvaz, D.; Nourry, A.; Davies, L.; Manne, H. A.; Lopes, F.; Preece, N.; Hedley, D.; Ogilvie, L. M.; Kirk, R.; Marais, R.; Springer, C. J. *J. Med. Chem.* **2010**, *53*, 5639; (c) Suijkerbuijk, B. M. J. M.; Niculescu-Duvaz, I.; Gaulon, C.; Dijkstra, H. P.; Niculescu-Duvaz, D.; Menard, D.; Zambon, A.; Nourry, A.; Davies, L.; Manne, H. A.; Friedlos, F.; Ogilvie, L. M.; Hedley, D.; Lopes, F.; Preece, N. P.; Moreno-Farre, J.; Raynaud, F. I.; Kirk, R.; Whittaker, S.; Marais, R.; Springer, C. J. *J. Med. Chem.* **2010**, *53*, 2741.
6. Smith, A. L.; DeMorin, F. F.; Paras, M. A.; Huang, Q.; Petkus, J. K.; Doherty, E. M.; Nixey, T.; Kim, J. L.; Whittington, D. A.; Epstein, L. F.; Lee, M. R.; Rose, M. J.; Babij, C.; Fernando, M.; Hess, K.; Le, Q.; Beltran, P.; Carnahan, J. *J. Med. Chem.* **2009**, *52*, 6189.
7. Carnahan, J.; Beltran, P. J.; Babij, C.; Le, Q.; Rose, M. J.; Vonderfecht, S.; Kim, J. L.; Smith, A. L.; Nagapudi, K.; Broome, M. A.; Fernando, M.; Kha, H.; Belmontes, B.; Radinsky, R.; Kendall, R.; Burgess, T. L. *Mol. Cancer Ther.* **2010**, *9*, 2399.

8. Wisler, J.; Afshari, C.; Fielden, M.; Zimmermann, C.; Taylor, S.; Carnahan, J.; Vonderfecht, S. *Toxicol. Pathol.* **2011**, *39*, 809.
9. (a) King, A. J.; Patrick, D. R.; Batorsky, R. S.; Ho, M. L.; Do, H. T.; Zhang, S. Y.; Kumar, R.; Rusnak, D. W.; Takle, A. K.; Wilson, D. M.; Hugger, E.; Wang, L.; Karreth, F.; Lougheed, J. C.; Lee, J.; Chau, D.; Stout, T. J.; May, E. W.; Rominger, C. M.; Schaber, M. D.; Luo, L.; Lakdawala, A. S.; Adams, J. L.; Contractor, R. G.; Smalley, K. S. M.; Herlyn, M.; Morrissey, M. M.; Tuveson, D. A.; Huang, P. S. *Cancer Res.* **2006**, *66*, 11100; (b) Hoeflich, K. P.; Herter, S.; Tien, J.; Wong, L.; Berru, L.; Chan, J.; O'Brien, C.; Modrusan, Z.; Seshagiri, S.; Lackner, M.; Stern, H.; Choo, E.; Murray, L.; Friedman, L. S.; Belvin, M. *Cancer Res.* **2009**, *69*, 3042; (c) Poulikakos, P.; Zhang, C.; Bollag, G.; Shokat, K. M.; Rosen, N. *Nature* **2010**, *464*, 427; (d) Hatzivassiliou, G.; Song, K.; Yen, I.; Brandhuber, B. J.; Anderson, D. J.; Alvarado, R.; Ludlam, M. C.; Stokoe, D.; Gloor, S. L.; Vigers, G.; Morales, T.; Aliagas, I.; Liu, B.; Siberis, S.; Hoeflich, K. P.; Jaiswal, B. S.; Seshagiri, S.; Koeppen, H.; Belvin, M.; Friedman, L. S.; Malek, S. *Nature* **2010**, *464*, 431; (e) Heidhorn, S. J.; Milagre, C.; Whittaker, S.; Nourry, A.; Niculescu-Duvas, I.; Dhomen, N.; Hussain, J.; Reis-Filho, J.; Springer, C. J.; Pritchard, C.; Marais, R. *Cell* **2010**, *140*, 209.
10. (a) Rajakulendran, T.; Sahmi, M.; Lefrançois, M.; Sicheri, F.; Therrien, M. *Nature* **2009**, *461*, 542; (b) Lavoie, H.; Thevakumaran, N.; Gavory, G.; Li, J. J.; Padeganeh, A.; Guiral, S.; Duchaine, J.; Mao, D. Y. L.; Bouvier, M.; Sicheri, F.; Therrien, M. *Nat. Chem. Bio.* **2013**, *9*, 428; (c) Lavoie, H.; Li, J. J.; Thevakumaran, N.; Therrien, M.; Sicheri, F. *Trends Biochem. Sci.* **2014**, *39*, 475.
11. Freeman, A. K.; Ritt, D. A.; Morrison, D. K. *Mol. Cell* **2013**, *49*, 751.
12. Le, K.; Blomain, E. S.; Rodeck, U.; Aplin, A. E. *Pigment Cell & Melanoma Research* **2013**, *26*, 509.
13. It should be pointed out that due to the lower affinity of B-Raf^{V600E} protein for ATP compared to that of B-Raf^{WT} protein (ratio of K_M ~13, see Ref. 9d) for a given compound, the value of ^{b}S derived from IC_{50}'s may be exaggerated than those based on K_i values. The [ATP] used for our biochemical assays were 10 μM for B-Raf^{V600E} protein and 1 μM for B-Raf^{WT} protein, respectively. However, for comparison purposes, the K_M difference will not affect the relative ranking order of compounds tested under the same conditions.
14. (a) Tsai, J.; Lee, J. T.; Wang, W.; Zhang, J.; Cho, H.; Mamo, S.; Bremer, R.; Gillette, S.; Kong, J.; Haass, N. K.; Sproesser, K.; Li, L.; Smalley, K. S. M.; Fong, D.; Zhu, Y.-L.; Marimuthu, A.; Nguyen, H.; Lam, B.; Liu, J.; Cheung, I.; Rice, J.; Suzuki, Y.; Luu, C.; Settachatgul, C.; Shellooe, R.; Cantwell, J.; Kim, S.-H.; Schlessinger, J.; Zhang, K. Y. J.; West, B. L.; Powell, B.; Habets, G.; Zhang, C.; Ibrahim, P. N.; Hirth, P.; Artis, D. R.; Herlyn, M.; Bollag, G. *Proc. Natl. Acad. Sci. U.S.A.* **2008**, *105*, 3041; (b) Ibrahim, P. N.; Artis, D. R.; Bremer, R.; Mamo, S.; Nespi, M.; Zhang, J.; Zhu, Y.-L.; Tsai, J.; Hirth, P.; Bollag, G.; Spevak, W.; Cho, H.; Gillette, S.; Wu, G.; Zhu, H.; Shi, S. WO 2007/002325 A1, 2006.; (c) Ibrahim, P. N.; Artis, D. R.; Bremer, R.; Habets, G.; Mamo, S.; Nespi, M.; Zhang, C.; Zhang, J.; Zhu, Y.-L.; Zuckerman, R.; West, B.; Suzuki, Y.; Tsai, J.; Hirth, P.; Bollag, G.; Spevak, W.; Cho, H.; Gillette, S.; Wu, G.; Zhu, H.; Shi, S. WO 2007/002433, 2006.; (d) Bollag, G.; Hirth, P.; Tsai, J.; Zhang, J.; Ibrahim, P. N.; Cho, H.; Spevak, W.; Zhang, C.; Zhang, Y.; Habets, G.; Burton, E. A.; Wong, B.; Tsang, G.; West, B. L.; Powell, B.; Shellooe, R.; Marimuthu, A.; Nguyen, H.; Zhang, K. Y. J.; Artis, D. R.; Schlessinger, J.; Su, F.; Higgins, B.; Iyer, R.; D'Andrea, K.; Koehler, A.; Stumm, M.; Lin, P. S.; Lee, R. J.; Grippo, J.; Puzanov, I.; Kim, K. B.; Ribas, A.; McArthur, G. A.; Sosman, J. A.; Chapman, P. B.; Flaherty, K. T.; Xu, X.; Nathanson, K. L.; Nolop, K. *Nature* **2010**, *467*, 596; (e) Flaherty, K. T.; Puzanov, I.; Kim, K. B.; Ribas, A.; McArthur, G. A.; Sosman, J. A.; O'Dwyer, P. J.; Lee, R. J.; Grippo, J. F.; Nolop, K.; Chapman, P. B. *N. Eng. J. Med.* **2010**, *363*, 809.
15. (a) Adam, J. L.; Dickerson, S. H.; Johnson, N. W.; Kuntz, K.; Petrov, K.; Ralph, J. M.; Rheaut, T. R.; Schaaf, G.; Stellwagen, J.; Tian, X.; Uehling, D. E.; Waterson, A. G.; Wilson, B.; WO 2009/137391, 2009.; (b) Rheault, T. R.; Stellwagen, J. C.; Adjabeng, G. M.; Hornberger, K. R.; Petrov, K. G.; Waterson, A. G.; Dickerson, S. H.; Mook, R. A.; Laquerre, S. G.; King, A. J.; Rossanese, O. W.; Arnone, M. R.; Smitheman, K. N.; Kane-Carson, L. S.; Han, C.; Moorthy, G. S.; Moss, K. G.; Uehling, D. E. *ACS Med. Chem. Lett.* **2013**, *4*, 358.
16. Su, F.; Viros, A.; Milagre, C.; Trunzer, K.; Bollag, G.; Spleiss, O.; Reis, J. S.; Kong, X. J.; Koya, R. C.; Flaherty, K. T.; Chapman, P. B.; Kim, M. J.; Hayward, R.; Martin, M.; Yang, H.; Wang, Q. Q.; Hilton, H.; Hang, J. S.; Noe, J.; Lambros, M.; Geyer, F.; Dhomen, N.; Niculescu-Duvaz, I.; Zambon, A.; Niculescu-Duvaz, D.; Preece, N.; Robert, L.; Otte, N. J.; Mok, S.; Kee, D.; Ma, Y.; Zhang, C.; Habets, G.; Burton, E. A.; Wong, B.; Nguyen, H.; Kockx, M.; Andries, L.; Lestini, B.; Nolop, K. B.; Lee, R. J.; Joe, A. K.; Troy, J. L.; Gonzalez, R.; Hutson, T. E.; Puzanov, I.; Chmielowski, B.; Springer, C. J.; McArthur, G. A.; Sosman, J. A.; Lo, R. S.; Ribas, A.; Marais, R. *N. Eng. J. Med.* **2012**, *366*, 207.
17. For a discussion on the binding modes of B-Raf inhibitors, see: Wang, X.; Kim, J. *J. Med. Chem.* **2012**, *55*, 7332.
18. (a) After the completion of our work, a patent describing sulfonamides was published that included some of the examples shown in this paper (**4** (**a**, **e**, **g**, **j**) and **5**(**a**, **b**, **d**, **h**, **k**–**m**, **o**): Shim, E. K.; Kim, N. D.; Shim, T. B.; Kim, S. Y. WO 2,012,074,249, 2012; US, 20,130,317,023, 2013.; (b) Kim, Y.-K.; Ahn, S. K.; Lee, M. *Cancer Lett.* **2012**, *320*, 215; (c) Ahn, J.-H.; Ahn, S. K.; Lee, M. *Biochem. Biophys. Res. Comm.* **2012**, *417*, 857; (d) A related patent including compounds **4**(**a**, **d**) and **5**(**a**, **b**, **c**) was published: Xiao, D.; Li, J.; Zhu, Y.; Hu, Y.; Wang, H.; Wang, Z.; Wang, Z.; Wei, Y.; Sun, Y.; Wu, Q.; Zhang, H.; Peng, Y.; Kong, F.; Sun, Y.; Luo, H.; Han, Y., WO 2,013,071,865, 2013.
19. Hanson, J. R.; Saberi, H. *J. Chem. Res.* **2004**, 699.
20. Wu, G.; Zhang, J. Zhu, Y.-L.; Zhang, C.; Ibrahim, P. N.; Shi, S.; Spevak, W.; Artis, D.; Tsai, J., WO 2,009,012,283, 2009.
21. Berredjem, M.; Winum, J.-V.; Toupet, L.; Masmoudi, O.; Aouf, N.-F.; Montero, J.-L. *Synth. Commun.* **2004**, *34*, 1653.
22. For an early report comparing SAR of aryl amides and aryl sulfonamides in the αC-helix region, see, Stellwagen, J.; Adjabeng, G.; Arnone, M.; Dickerson, S.; Han, C.; Hornberger, K.; King, A.; Mook, R.; Petrov, K.; Rheault, T.; Rominger, C.; Rossanese, O.; Smitheman, K.; Waterson, A.; Uehling, D. *Bioorg. Med. Chem. Lett.* **2011**, *21*, 4436.
23. (a) Ref. 9d.; (b) Nakamura, A.; Arita, T.; Tsuchiya, S.; Donelan, J.; Chouitar, J.; Carideo, E.; Galvin, K.; Okaniwa, M.; Ishikawa, T.; Yoshida, S. *Cancer Res.* **2013**, *73*, 7043; (c) Okaniwa, M.; Hirose, M.; Arita, T.; Yabuki, M.; Nakamura, A.; Takagi, T.; Kawamoto, T.; Uchiyama, N.; Sumita, A.; Tsutsumi, S.; Tottori, T. *J. Med. Chem.* **2013**, *56*, 6478.
24. The calculated pK_a (ACD/Labs) for the sulfamide NH in **6a** is ~7.3, about 0.5-unit lower than the value estimated for sulfonamide **5h**.
25. (a) Mathieu, S.; Gradl, S. N.; Ren, L.; Wen, Z.; Aliagas, I.; Gunzner-Toste, J.; Lee, W.; Pulk, R.; Zhao, G.; Alicke, B.; Boggs, J. W.; Buckmelter, A. J.; Choo, E. F.; Dinkel, V.; Gloor, S. L.; Could, S. E.; Hanson, J. D.; Hastings, G.; Hatzivassiliou, G.; Laird, E. N.; Moreno, D.; Ran, Y.; Voegtli, W. C.; Wenglowsky, S.; Grina, J.; Rudolph, J. *J. Med. Chem.* **2012**, *55*, 2869; (b) Wenglowsky, S.; Ren, L.; Ahrendt, K. A.; Laird, E. R.; Aliagas, I.; Alicke, B.; Buckmelter, A. J.; Choo, E. F.; Dinkel, V.; Feng, B.; Gloor, S. L.; Gould, S. E.; Gross, S.; Gunzner-Toste, J.; Hansen, J. D.; Hatzivassiliou, G.; Liu, B.; Malesky, K.; Mathieu, S.; Newhouse, B.; Raddatz, N. J.; Ran, Y.; Rana, S.; Randolph, N.; Risom, T.; Rudolph, J.; Savage, S.; Selby, L. T.; Shrag, M.; Song, K.; Sturgis, H. L.; Voegtli, W. C.; Wen, Z.; Willis, B. S.; Woessner, R. D.; Wu, W.-I.; Young, W. B.; Grina, J. *ACS Med. Chem. Lett.* **2011**, *2*, 342; (c) Wenglowsky, S.; Ren, L.; Grina, J.; Hansen, J. D.; Laird, E. R.; Moreno, D.; Dinkel, V.; Gloor, S. L.; Hastings, G.; Rana, S.; Rasor, K.; Sturgis, H. L.; Voegtli, W. C.; Viers, G.; Willis, B.; Mathieu, S.; Rudolph, J. *Bioorg. Med. Chem. Lett.* **2014**, *24*, 1923. and references cited therein.
26. Thevakumaran, N.; Lavoie, H.; Critton, D. A.; Tebben, A.; Marinier, A.; Sicheri, F.; Therrien, M. *Nat. Struct. Mol. Biol.* **2015**, *22*, 37.
27. Molecular dynamics simulation studies also revealed distinct changes in the A-loop and αC-helix regions of B-Raf protein complexed to linear and branched sulfonamides. Arora, R.; Michele, M. D.; Stes, E.; Vandermarliere, E.; Martens, L.; Gevaert, K.; Heerde, E. V.; Linders, J. T. M.; Brehmer, D.; Jacoby, E.; Bonnet, P. *J. Med. Chem.* **2015**, *58*, 1818.
28. Zhang, C.; Spevak, W.; Zhang, Y.; Burton, E. A.; Ma, Y.; Habets, G.; Zhang, J.; Lin, J.; Ewing, T.; Matusow, B.; Tsang, G.; Marimuthu, A.; Cho, H.; Wu, G.; Wang, W.; Fong, D.; Nguyen, H.; Shi, S.; Womack, P.; Nespi, M.; Shellooe, R.; Carias, H.; Powell, B.; Light, E.; Sanftner, L.; Walters, J.; Tsai, J.; West, B. L.; Visor, G.; Resaei, H.; Lin, P. S.; Nolop, K.; Ibrahim, P. N.; Hirth, P.; Bollag, G. *Nature* **2015**, *526*, 583.
29. Otwinowski, Z.; Minor, W. *Methods Enzymol.* **1997**, *276*, 307.
30. Kissinger, E. R.; Gehlhaar, D. K.; Fogel, D. B. *Acta Crystallogr., Sect. D* **1999**, *55*, 484.
31. Murshudov, G. N.; Vagin, A. A.; Dodson, E. J. *Acta Crystallogr., Sect. D* **1997**, *53*, 240.
32. Collaborative Computational Project, No. 4 The CCP4 Suite: Programs for crystallography. *Acta Crystallogr., Sect. D* **1994**, *50*, 760.
33. Emsley, P.; Cowtan, K. *Acta Crystallogr., Sect. D* **2004**, *60*, 2126.
34. Kuramoto, Y.; Ohshita, Y.; Yoshida, J.; Yazaki, A.; Shiro, M.; Koike, T. *J. Med. Chem.* **2003**, *46*, 1905.